Agricultural and Forest Meteorology 164 (2012) 96–111

Contents lists available at SciVerse ScienceDirect

Agricultural and Forest Meteorology

journal homepage: www.elsevier.com/locate/agrformet

Assessing climate change effects on European crop yields using the Crop Growth Monitoring System and a weather generator

I. Supit[a,*], C.A. van Diepen[b], A.J.W. de Wit[b], J. Wolf[d], P. Kabat[a,e], B. Baruth[c], F. Ludwig[a]

[a] Earth System Science & Climate Change, Wageningen University and Research Centre, P.O. Box 47, 6700 AA Wageningen, The Netherlands
[b] Center for Geo Information, Alterra, Wageningen University and Research Centre, P.O. Box 47, 6700 AA Wageningen, The Netherlands
[c] Plant Production Systems Group, Wageningen University and Research Center, P.O. Box 430, 6700 AK Wageningen, The Netherlands
[d] IES, Joint Research Centre of EC, Via E. Fermi 2749, 21027 Ispra (VA), Italy
[e] International Institute for Applied Systems Analysis (IIASA), Laxenburg, Austria

ARTICLE INFO

Article history:
Received 1 July 2011
Received in revised form 19 April 2012
Accepted 10 May 2012

Keywords:
Climate change
Crop yields
Winter wheat
Maize
Potato
Sugar beet

ABSTRACT

Climate change impacts on potential and rainfed crop yields on the European continent were studied using output of three General Circulation Models and the Crop Growth Monitoring System in combination with a weather generator.

Climate change impacts differ per crop type and per CO_2 emission scenario. Crops planted in autumn and winter (winter wheat) may benefit from the increasing CO_2 concentration. Rainfall is sufficient and if the CO_2 concentration increase is high, yields may increase up to 2090. If the CO_2 increase is less, increasing temperatures result in declining or stagnating yields after 2050.

Crops planted in spring (potato, sugar beet) initially benefit from the CO_2 increase, however as time progresses the increasing temperatures reduce these positive effects. By the end of the century yields decline in southern Europe and production may only be possible if enough irrigation water is available. In northern Europe depending on the temperature and CO_2 concentration increase, yields either stagnate or decline. However in some of the cooler regions yield increase is still possible.

Crops planted in late spring and summer (maize) may suffer from droughts and high temperature in summer. By the end of the century, depending on the temperature rise, crop yields decline almost everywhere. If the temperature increase is less only in north western Europe yields remain stable.

1. Introduction

Agricultural production is greatly affected by climate and changes in greenhouse gas concentrations, radiation and temperature patterns may have large consequences for the potential and rainfed yields. Except in the coolest regions where the temperature is currently below the optimum range, rising temperatures may affect crop production negatively, the growing season is shortened and the time for biomass accumulation is reduced (e.g. Lobell and Field, 2007; Battisti and Naylor, 2009; Giannakopoulos et al., 2009; Supit et al., 2010b). The elevated atmospheric CO_2 concentration may increase production for various crops (e.g. Miglietta et al., 1998; Qaderi and Reid, 2005; Franzaring et al., 2008). For example, Amthor (2001) compared 50 studies on the effects of CO_2 concentration on wheat. He concluded that doubling of the CO_2 concentration from 350 to 700 ppm increased wheats yield with 31%, provided ample nutrients and water are available. However, yield increases in free air CO_2 enrichment (FACE) studies are lower than for enclosure studies (Long et al., 2006). Furthermore, a modest warming trend (1–4 °C) will counteract the positive effects of a doubled CO_2 concentration (Amthor, 2001).

Biophysical models are commonly used to estimate plant growth and production (e.g. Brown and Rosenberg, 1997; Easterling et al., 2001; Parry et al., 2004; Ewert et al., 2005). These models can also be used to evaluate climate change impacts on crop development, growth and yield by combining future climate conditions, obtained from General or Regional Circulation Models (GCMs and RCMs respectively), with the simulation of CO_2 physiological effects, derived from FACE studies (Moriondo et al., 2010; Asseng et al., 2004). In this study we used the Crop Growth Monitoring System (CGMS) of the European Commission (http://mars.jrc.it/mars/About-us/AGRI4CAST/Crop-yield-forecast/The-Crop-Growth-Monitoring-System-CGMS).

CGM outputs are freely available from the IPCC Data Distribution Centre (www.ipcc-data.org) and can be used by the research community to assess climate change impacts on for example agricultural crops and natural ecosystems, biodiversity and plant diseases (Semenov and Stratonovitch, 2010). We used the CMIP3 multi-model results (Meehl et al., 2007) that are produced by various research groups, who coordinated the climate experiments,

* Corresponding author. Tel.: +31 317 486585.
E-mail address: iwan.supit@wur.nl (I. Supit).

0168-1923/$ – see front matter © 2012 Elsevier B.V. All rights reserved.
http://dx.doi.org/10.1016/j.agrformet.2012.05.005

Table 1
Models used in this study.

Model name	Modeling group	Country	References
IPSL-CM4	Institute Pierre Laplace	France	Dufresne (2007a,b,c)
MICRO3.2	Center for Climate System Research	Japan	Nozawa (2005a,b,c)
ECHAM5/MPI-OM	Max-Planck Institute for Meteorology	Germany	Roeckner (2005, 2006, 2007)

i.e. several GCMs were run for a common set of experiments and various emissions scenarios (Solomon et al., 2007). The models we used are referenced in Table 1.

General and regional climate model results cannot directly be used as input for biophysical models because the output is typically available as monthly means or changes in monthly means of climatic variables (Semenov and Stratonovitch, 2010) and most biophysical models need daily time series as input. Even if daily output is available, the coarse spatial resolution and large biases, in particular for precipitation make the output unsuitable for direct use (Semenov, 2007; Semenov and Stratonovitch, 2010).

Through scaling a standard gridded data set of mean weather variables from a predefined baseline range of weather variables (New et al., 2000) with differences between current and future conditions can be obtained (Alcamo et al., 2007). This approach however, considers only the changes in the mean, it does not account for the variability. Extreme values in future climate scenarios are leveled off (Graham et al., 2007). To tackle this problem crop modelers often use bias correction methods that apply transfer functions from observed and simulated cumulative distribution functions (e.g. Ines and Hansen, 2006). These methods are given a wide range of names in the literature: statistical downscaling, quintile mapping, histogram equalizing, and rank matching are among these (Piani et al., 2009). Alternatively, daily site-specific climate scenario datasets can be created using a stochastic weather generator (Wilks, 1992; Barrow and Semenov, 1995; Wilks and Wilby, 1999; Semenov, 2007), but this requires that the mathematical parameters for the generator are known. In this study we used a weather generator (Section 3.1).

Sowing and planting dates, crop responses to the changing temperature and radiation patterns, water shortages, interact in a non-linear way may lead to different trends per crop and per region. To have a clear impression of climate change impacts on agricultural production we selected four crops that are extensively cultivated in Europe and that differ in respect to their sowing date (winter vs. spring/summer crops), response to changing CO_2 concentrations and response to changing temperatures (C3 vs. C4 crops). We selected winter wheat to represent winter crops, sugar beet and potato to represent the spring root crops and maize to represent a spring/summer C4 grain crop. We assumed that planting dates do not change in time.

We investigated the future potential and rainfed yields in the years 2030, 2050 and 2090.

2. Data

2.1. GCM data

We used the IPCC AR4 GCM simulation results as future climate data. Note that the range of these simulation results is large and regionally dependent (NRC, 2003; Giorgi and Bi, 2005) and therefore we used data from three GCMs and two emission scenarios (A2 and B1) mentioned in the Special Report on Emissions Scenarios (Nakićenović et al., 2000) (Table 1). These particular GCMs were selected because daily temperature and rainfall data were available for all model simulations. In addition, these GCMs showed a reasonable match between observed and simulated temperature and rainfall (Hagemann et al., 2011). Each of the selected GCM's deal with climatological feedbacks in different ways and it is broadly assumed that the average of various GCM's provides the best representation of future climate. The emission scenarios represent different mixes of population changes, economic output, land use, energy and technology use and can be generally characterized by maximum atmospheric CO_2 concentrations (Sheffield and Wood, 2007). A2 represents the worst-case scenario. As a result of continuously increasing global population and limited technological change, CO_2 emissions in the period 2000–2099 will multiply 4–5 times and the atmospheric CO_2 concentrations will increase from about 350 to 850 ppm. Temperature increases 2.0–5.4 °C. In the B1 scenario environmental protection is emphasized and world population increases relatively slow. The atmospheric CO_2 concentrations will stabilize at 550 ppm by the end of the century. Temperature increases 1.1–2.9 °C. We also used data from the twentieth century simulations (20C3M). These simulations are dictated by historical greenhouse gas and sulfate-aerosol concentrations and other forcing's since the start of the industrial revolution (Sheffield and Wood, 2007). Where ensemble simulations for a particular scenario were available we used the first ensemble.

2.2. MARS CGMS data

2.2.1. Historical gridded weather data

Historical weather data are taken from the MARS-STAT Data Base provided by the Monitoring Agricultural Resources (MARS) Unit of the Institute for Environment and Sustainability of the Joint Research Centre of the European Commission at Ispra, Italy. These data consist of daily values of maximum and minimum temperatures, wind speed, global radiation and vapor pressure, rainfall, interpolated from station data to a 50 × 50 km climatic grid (Beek et al., 1992; van der Voet et al., 1993; Micale and Genovese, 2004). Our study area covers 5014 grid cells. Weather data have been collected from the Global Telecommunication System (GTS) of the World Meteorological Organization as well as from national and sub national station networks. Presently, data from nearly 7000 stations is available. Of these stations about 2500 receive daily meteorological information. Missing global radiation values are computed automatically from data from the GTS: sunshine duration, a combination of cloudiness and the temperature range or only the temperature range. Other missing data are replaced by long term average values. From 1976 a more or less complete European coverage is available.

2.2.2. Crop data and administrative regions

Per region and per crop various varieties are cultivated. Per region, for all crops of interest, crop calendars of the regional crop varieties have been collected, including sowing dates of sowing, flowering, and maturity or harvest. For non-flowering root crops the start of tuber formation was collected, and for some crops that may not reach maturity (i.e. sugar beet, potato, and maize) the end of season as well. Based on this information, per region and per crop, a crop file has been constructed that describes the growth and development of an average crop variety. For each crop–region combination a fixed sowing date and a fixed crop parameter set are assumed. The present study covers crop information for 372 NUTS2 regions. This information is based on the research Boons-Prins et al.

(1993), Russell and Wilson (1994), Carbonneau et al. (1992), Falisse (1992), Narciso et al. (1992), Bignon (1990), Falisse and Decelle (1990), Hough (1990) and Russell (1990). Since new crop varieties are constantly introduced, crop parameters that describe crop growth and development are regularly updated and calibrated (e.g. Gisat, 2003; Willekens et al., 1998a,b).

2.2.3. Soil data and cultivated area

Soil properties such as texture, rootable soil depth, slope and agricultural limiting phase (due to presence of stones, cemented layers, rocks, erosion etc.) are available from the 1 to 1 million soil map, version 3.1 (INRA, 1995; Le Bas, 1996; Jones and Buckley, 1996). Texture and rooting depth determine the water availability. Rooting depth, drainage conditions, salinity and alkalinity are derived from basic soil properties using pedotransfer rules (Lazar and Genovese, 2004). Detailed crop maps on the exact cultivated locations are not available. Therefore the soil map is used to construct a proxy land use map, by assuming that in all regions where a given crop is grown, this crop is cultivated on all soils judged suitable. For the suitability assessment each crop is assigned to one of the following groups: grasses, cereals and root crops, of which the root crops are the most demanding in terms of soil quality. The requirements per crop group with respect to soil related characteristics such as rootable soil depth, agricultural limiting phase, drainage, presence of stones, texture, alkalinity and salinity is accounted for and differ per crop group. Missing planted area values for NUTS2-administrative region level (used in the aggregation procedure) are replaced with long term average values. Note that in the baseline and all future situations the same cultivated area has been applied, while we may expect some shifts in cultivated area from one region to another, in response to the changes in climatic suitability for a given crop.

2.3. Spatial schematization

Simulations are performed per simulation unit which is an area mapped as an unique combination of a climatic grid cell and Soil Typological Unit (STU) and valid for a given crop. The size of simulation unit varies between 210 and 360 km^2. A STU is located in one or more Soil Mapping Units (SMU) and the proportion of the SMU area occupied by each STU is known. Model input and output are also related to administrative regions through the EMU + NUTS intersection, where EMU stands for the Elementary Mapping Unit which is the intersection of a climatic grid cell and a SMU. Consequently, the location and area extent of given simulation unit can be related to the grid, SMU and administrative region. Simulation results (in ton/ha) are subsequently aggregated to mean values per NUTS2, NUTS1 and NUTS0 level using the following equation:

$$S_h = \frac{\sum_{i=n}^{n} A_i S_i}{\sum_{i=n}^{n} A_i} \tag{1}$$

where S_h is the simulation result at a higher level, S_i the simulation result at a lower level and A_i the total area deemed suitable for a specific crop within a NUTS2 region. For subsequent aggregation steps the same equation is applied. As land use information on NUTS2-level comes available, usually 1 or 2 years after the season ends, observed A_i values are used. For the scenario simulations we used A_i values of 2008.

3. Methods

We used two scenario sets from each of the three different GCM's. We also used the outputs of the "climate of the 20th Century experiment" (20C3M) that describe the climate for the period 1st January 1970 until 31st December 1999. We only used the period 1st January 1980 until 31st December 1999. Differences between the scenarios and the 20C3M series are used to adapt the parameters of a weather generator. In a next step, 31 years of synthetic daily weather data are generated which are subsequently introduced in the CGMS crop modeling procedure. The results are compared with results obtained with observed weather data for the period 1990–2008 (baseline).

3.1. Weather generation

3.1.1. Model development

3.1.1.1. Rainfall occurrence. Rainfall occurrence can be modeled using the first order, two-state Markov process (e.g. Todorovic and Woolhiser, 1975; Katz, 1977; Stern and Coe, 1984; Wilks, 1998). However according to Racsko et al. (1991) the length of dry and wet series, parameters that are important for plant growth and development, cannot be approximated closely from this model, and semi-empirical distributions perform better. Therefore in our study we used the method applied in the LARS weather generator (Semenov and Barrow, 1997; Semenov et al., 1998; Semenov and Brooks, 1999). We use a histogram Emp = $\{a_0, a_i; h_i, i = 1,\ldots,10\}$ with 10 intervals $[a_{i-1}, a_i]$, where $a_{i-1} < a_i$, and h_i denotes the number of events from the observed data in the i-th interval. Random values from the semi-empirical distributions are chosen by first selecting one of the intervals (using the proportion of events in each interval as the selection probability), and subsequently a value is selected. A uniform distribution within that interval is assumed.

3.1.1.2. Selection of best fitting distribution for precipitation amounts. Precipitation amounts are often modeled using a two-parameter gamma distribution (Katz, 1977; Buishand, 1978; Richardson, 1981). Other distributions that can be applied are the exponential distribution (Todorovic and Woolhiser, 1975), Weibull distribution (Sharda and Das, 2005), and two so-called mixed distributions, the mixed exponential distribution (Woolhiser and Roldan, 1982; Foufoula-Georgiou and Lettenmaier, 1987; Chapman, 1997, 1998; Wilks, 1999) and the mixed Weibull distribution (Suhaila and Jemian, 2007). Prior to this study we fitted the above mentioned distributions to the CGMS grid cell rainfall series. Subsequently we compared the goodness of fit using Kolmogorov–Smirnov test. The mixed distributions provided substantially better fits and of the two tested mixed distributions, the mixed Weibull performed best. In this study the parameters are estimated on a monthly basis.

Mixed Weibull distribution to generate precipitation amounts:

$$f(x) = p\left(\frac{\alpha 1}{\beta 1}\right)\left(\frac{x}{\beta 1}\right)^{\alpha 1-1}\exp\left[-\left(\frac{-x}{\beta 1}\right)^{\alpha 1}\right] + (1-p)\left(\frac{\alpha 2}{\beta 2}\right)\left(\frac{x}{\beta 2}\right)^{\alpha 2-1}\exp\left[-\left(\frac{-x}{\beta 2}\right)^{\alpha 2}\right] \tag{2}$$

$$0 \le p \le 1, \quad \alpha > 0, \quad \beta > 0, \quad x > 0$$

where α1,2 and β1,2 are the shape and scale parameters respectively and p is the mixing factor.

3.1.1.3. Temperature, radiation and vapor pressure. The procedure to generate time series of minimum and maximum temperatures, radiation and vapor pressure as described by Richardson (1981) is based on the weakly stationary generating process given by Matalas (1967):

$$R_t = [A]R_{t-1} + [B]e_i \tag{3}$$

R_t and R_{t-1} are 4×1 matrices for day t whose elements are standardized residuals (zero mean, unit variance) of radiation, vapor pressure, maximum, and minimum temperature values for days t and $t-1$, respectively. These standardizations are conditional on wet or dry days. e_i is a vector of independent random components. The parameter matrices $[A]$ and $[B]$ are 4×4 matrices whose elements are defined such that the new sequences have the desired serial-correlation and cross-correlation. These matrices are calculated from lagged and unlagged correlations for the conditionally standardized variables (Richardson, 1981). Daily generated values are obtained by:

$$X_t = m(R_t c + 1) \quad (4)$$

where m is the monthly mean and c the coefficient of variation. The monthly change in means and coefficient of variation in a year can be described by:

$$m = \overline{m} + A \cos\left(\frac{2\pi(t-T)}{365}\right) \quad (5)$$

where A is the annual amplitude and T is the day determining the position of the harmonic.

3.1.1.4. Wind speed. A variety of parametric probability distribution functions to describe wind speed frequency distributions have been proposed. Currently, the two-parameter Weibull distribution is most widely used (Tuller and Brett, 1984). A two-component mixture Weibull distribution is able to represent heterogeneous wind. However, several authors (Burton et al., 2001; Jaramillo and Borja, 2004; Ramírez and Carta, 2006) as cited by Carta and Ramírez (2007) have indicated that the Weibull distribution should not be used in a generalized way, as it is unable to represent some wind regimes which show bimodality or bitangentiality. Similar to Jaramillo and Borja (2004) and Carta and Ramírez (2007), we used a mixed Weibull distribution to represent wind regimes. We assume that wind speed is independent from the other parameters.

3.1.2. Generating time series of future weather data

The time slices 1980–2000, 2020–2040, 2040–2060 and 2080–2100 were chosen from the GCM data. Average differences between the period 1980–2000 and future time slices were used to adapt the parameters of the weather generator. For every grid cell the parameters are established. It is assumed that these newly created parameters represent the weather patterns in respectively 2030, 2050 and 2090. For each of these years 31 complete sets of daily weather data are generated. This was done for all six parameter sets derived from the two emission scenarios and the three GCM models.

3.2. CGMS crop growth modeling procedure

3.2.1. Model and aggregation of output

This paper presents other aspects of the research published earlier in Supit et al. (2010a,b). Similar to these papers, we used the Crop Growth Monitoring System (GCMS) version 8.1.2. to assess the crop yields across Europe. CGMS is the monitoring system used by the AGRI4CAST department of the MARS Unit of the European Commission to monitor and assess crop yields. Detailed information on CGMS can be found at http://mars.jrc.it/mars/Projects/Methodology-of-the-MARS-Crop-Yeld-Forecasting-Systems-METAMP. How CGMS results are used can be seen at: http://mars.jrc.it/mars/Bulletins-Publications. CGMS applies the WOFOST crop growth simulation model. Its underlying principles have been discussed by van Keulen and Wolf (1986). The initial version of this model was developed by the Centre for World Food Studies in Wageningen (Diepen et al., 1988; van Diepen et al., 1989). Implementation in CGMS and its structure is described by Supit et al. (1994) a standalone of WOFOST is described by Boogaard et al. (1998). Two production situations are simulated: potential and rainfed. The potential crop production situation is defined by temperature, day length, solar radiation and crop characteristics. Optimum nutrient and moisture levels are assumed. We used the potential simulation results to research the effects of the changing temperature and global radiation patterns on the yield potential of various crops. The rainfed situation is defined by the same parameters as the potential situation, in addition the soil moisture status is considered as well. It is used to research to examine the effects of drought on crop yield.

CGMS uses the administrative regions of the European Union, the so-called NUTS regions (http://epp.eurostat.ec.europa.eu/portal/page/portal/nuts_nomenclature/introduction). Four NUTS levels can be distinguished, however in CGMS only three are used: the national level (NUTS0), the regional level (NUTS1) and the sub-regional level (NUTS2).

Simulated leaf area index values, water requirement, water consumption, dry matter production per hectare, etc., are aggregated to sub-regional level (NUTS2), regional level (NUTS1) and finally to national level (NUTS0). In the present study we focus on final crop yield. Specifically, the aggregated yield data in this pan-European study originate from simulations over 31 years and all the simulation units, for both baseline and three future periods, using three GCMs per future scenario. The aggregated yields and their changes in three time steps over the 21 century will be discussed per crop, for two yield levels and two scenarios, using a table showing yields on country level, and a map showing yield changes on NUTS2-level. The procedure to aggregate the simulation results to regional and subsequently to national level is briefly described in Section 2.2, in Supit et al. (2010a) a more detailed description can be found. In situations where the cropped area is evenly distributed over a country, and where yield changes follow the same trend, the aggregated figures at NUTS2 and at country level are similar. In case the cropped area within a country is concentrated in one or two sub-regions, or when the yield trends differ between NUTS2 regions, the national aggregated figures may seem to contradict the visual image on the map.

3.2.2. Incorporating changing atmospheric CO_2 concentrations

For the present situation we assumed a mean CO_2 concentration of 355 ppm. For the future we used the CO_2 concentrations from the ISAM reference model (http://www.grida.no/publications/other/ipcc_tar/). For the A2 scenario we used respectively 457, 552, and 771 ppm CO_2 for 2030, 2050 and 2090. For the B1 scenario we used respectively 437, 488 and 545 ppm CO_2.

3.2.2.1. C_4-crops. For C_4 plants such as maize (and other tall tropical grasses) the photosynthetic response to CO_2 is only very steep for atmospheric CO_2 concentrations well below the current level. In the present and also the future range of atmospheric CO_2 concentrations (e.g., 300–1000 μmol/mol), the rate of CO_2 assimilation practically does not change at increasing CO_2, even under high light intensities (Goudriaan and Unsworth, 1990). The transpiration rate of maize however, strongly decreases. Literature reviews by Cure (1985) and Cure and Acock (1986) indicate a stomatal conductance reduction of 40% and a transpiration decrease of 28% for maize at doubled atmospheric CO_2 and high light conditions. The transpiration reduction by maize at doubled CO_2 was calculated in a study with a stratified micrometeorological model (Goudriaan, 1977; Chen, 1984). A reduction of the stomatal conductance with 45% at doubled CO_2 resulted in a transpiration reduction of 26% if both the effects of increasing leaf temperature and decreasing air humidity in the canopy were taken into account (Goudriaan and Unsworth, 1990). As this micrometeorological feedback is not included in the method applied in CGMS to calculate the

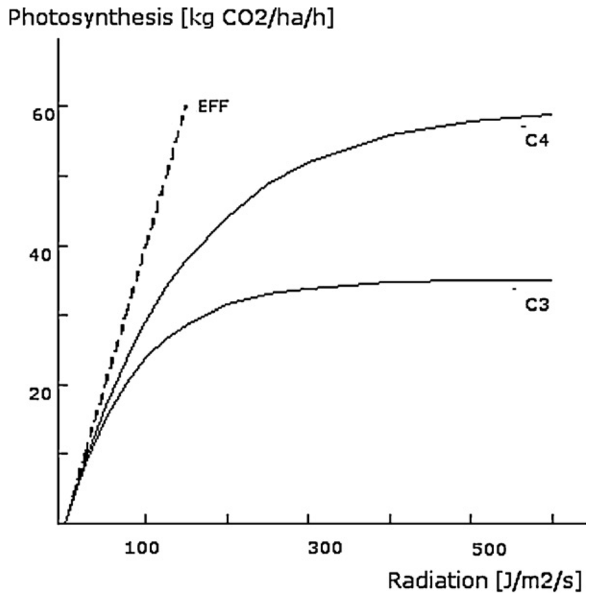

Fig. 1. Photosynthesis–light response curves of individual leaves for a C3 and a C4 crop, with a maximum of 40 and 60 kg ha^{-1} h^{-1}, respectively and both with Eff = 0.45 kg ha^{-1} h^{-1}/J m^{-2} s^{-1}. Measured at 340 ppm CO_2 and the maximum at optimum temperatures and Eff at a low temperature.
Data from Penning de Vries et al. (1989).

transpiration rate, the calculated transpiration rates are reduced by an overall factor. This reduction factor increases with increasing CO_2 and was set at 26% for a doubled CO_2 concentration (i.e., increase by 355 μmol/mol).

3.2.2.2. C$_3$-crops. Direct effects of the increasing atmospheric CO_2 concentration on the CO_2 assimilation and growth of C_3 crops are incorporated via the maximum and initial angle of the CO_2 assimilation–light response and a small decrease in transpiration rate. An example of an assimilation–light response is presented in Fig. 1. In this study the initial angle changes from 0.45 to 0.50 kg ha^{-1} h^{-1}/J m^{-2} s^{-1} and the maximum changes from 40 to 64 kg ha^{-1} h^{-1} as the CO_2 concentration increases from 355 μmol/mol in the present situation to 710 μmol/mol in 2090. The transpiration decreases 10% in the same period. Values for the other CO_2 concentrations applied in this study can be obtained through interpolation. These parameter adaptations are based on studies by Allen et al. (1990), Goudriaan et al. (1984, 1985), Goudriaan (1990), Goudriaan and Unsworth (1990), Goudriaan and de Ruiter (1983) and Idso (1990), and on literature surveys on crop responses to CO_2 doubling by Cure (1985), Cure and Acock (1986), and Kimball (1983). Pot experiments demonstrated that doubling the CO_2 concentration resulted in yield increases of 40–60%. However, yield increases in free air CO_2 enrichment (FACE) studies are lower than for enclosure studies (Long et al., 2006) due to more plant interaction (e.g. shadowing in canopy). Yield increases of 25–40% for doubled CO_2 (De Temmerman et al., 2002; Wolf and van Oijen, 2002, 2003; Wolf et al., 2002) were found in such circumstances.

Table 2
Lower threshold and upper cut off temperatures.

Crop	Lower threshold temperature (°C)	Upper cut off temperature (°C)
Winter wheat	0	30
Maize	6	30
Sugar beet	3	21
Potato	2	30

3.2.3. Crop development, photosynthesis, and yield formation

Phenological crop development is controlled by the daily mean temperature sum above a minimum threshold value. Similarly, a maximum cut off value is defined to put a ceiling to the daily increase in temperature sum. Higher temperatures shorten the length of successive phenological stages and consequently the total crop cycle. The lower threshold and maximum cut off values are crop specific and are given in Table 2 for the crops used in this study. Photosynthesis is a function of the global radiation. Outside a range of optimum temperatures the photosynthesis is corrected by a reduction factor to account for too high or for too low daily average temperatures. Table 3 presents the temperatures at which the photosynthesis at light saturation is optimum, zero and reduced to 50%. After subtracting maintenance respiration, assimilates are partitioned over roots, stems, leaves and grains as a function of the development stage. The maintenance respiration requirements increase during the crop's life time and in the final crop stages may take some 25–40% of the total assimilates for annual crops. The maintenance respiration requirements double for every 10 °C temperature increase. The growth respiration quantifies the conversion efficiency of transforming assimilates into structural plant dry matter.

3.2.4. Limitations

CGMS assumes that weeds, diseases, and pests are controlled and nutrients are optimally available. No information about future crop varieties is available and therefore we assume that crop types do not change over time. This will show the effects of the changing weather patterns on crop growth and production. Also plants ability to adapt to low resource conditions by modifying its morphology and physiology is not accounted for and simulated drought effects may therefore be more severe than they in reality are. Sowing date variations or occurrence of re-sowing in response to droughts may occur at regional and even national scale, however, since no information on these phenomena is available, for the spring and summer crops an average sowing date per crop and per region is assumed. Speculating that sowing starts earlier as a result of increasing temperatures, CGMS may overestimate sowing dates in the investigated periods. However, since emergence is temperature dependent, higher temperatures will result in an earlier emergence, thus partly reducing the effect of a late sowing date. Note that a correct sowing date is important. van der

Table 3
Temperatures at which the photosynthesis at light saturation is optimum, zero and reduced to 50%.

Crop	Low temp where assim = 0 (°C)	Lower limit optimum range for assim (°C)	Upper limit optimum range for assim (°C)	Temp. where assim is reduced by 0.5 (°C)	High temp. where assim = 0 (°C)
Winter wheat	0	15	25	30	35
Maize	9	20	30	>42	
Sugar beet	3	15	20	>40	
Potato	3	15	20	29	33

Assim = assimilation at light saturation.

Table 4
Percentage of grid cells where the mean and the variance of the simulated and observed parameters do not significantly differ ($p = 0.01$).

	Jan	Feb	Mar	Apr	May	Jun	Jul	Aug	Sep	Oct	Nov	Dec
Precipitation	97	99	91	96	99	88	88	97	97	78	99	97
Wind speed	97	98	96	96	92	91	89	89	92	95	96	97

Table 5
Second column: percentage of grid cells where the mean and the variance of the simulated and observed parameters do not significantly differ ($p = 0.01$). Third column: average mean bias error.

Maximum temperature	72	0.01	°C
Minimum temperature	68	−0.02	°C
Vapor pressure	66	−0.02	hPa
Global radiation	56	10.00	$KJ\,m^{-2}\,day^{-1}$

Table 6
Percentage of grid cells where the mean and the variance of the parameter simulated with the original data and those simulated with the generated weather data do not significantly differ ($p = 0.01$).

	Wheat	Maize	Sugar beets	Potato
Potential yield	94	91	90	90
Water limited yield	93	95	84	91

Wal (1995) showed that sugar beet simulation in the Netherlands using the observed sowing dates instead of the fixed mean optimum sowing date improved the regression between simulated and observed yields significantly. Vernalization and cold requirements (winter crops) are not accounted for. Development of the winter crops starts after a certain temperature sum calculated from the first of January is reached. Other weather factors not accounted for are water logging, frost, wind damage and erosion. These factors may be important at local scale, however, at a regional scale their effects on the year to year yield and biomass production variability are less important (van Diepen and van der Wal, 1995).

Irrigation practices may change in time, dictated by market developments, environmental regulations, etc. We did not consider irrigation, only the maximum (potential) and the rainfed situation are considered. In reality, in those areas where supplementary irrigation is applied, the actual yields will be higher than the calculated rainfed yields.

As the climate changes some crops types may not be cultivated anymore while new crop types will be introduced. We assumed that the crop types do not change over time. This shows how climate change affects crop growth and development over time.

4. Results

For each CGM and each emission scenario we executed crop simulations. For further analyses we averaged the simulation results per emission scenario. It is assumed that average values provide a realistic representation of the climate change effects on the studied crops. In the supplementary material average values and standard deviations of the simulated dry matter yields are presented per time slice, per CGM and per emission scenario. Variation among the time slices and among the GCM's are of the same magnitude. Difference among the CGM's is caused by the different feedback mechanism's applied in each model.

4.1. Simulation of historic weather patterns

Tables 4 and 5 present the percentage of grid cells where the mean and variance of the simulated and observed meteorological parameters do not significantly differ (t-test, $p < 0.01$). Monthly rainfall and wind speed distribution function are established and subsequently tested. In more than 90% of the grid cells the rainfall amounts and wind speed can be considered drawn from the same distribution (Table 4). Overall, the best fits are found for the period November–May, and somewhat less good fits in June–July. Only for rainfall in October the fit is below 80%. Based on Table 4 one can conclude that the mixed Weibull distribution can be used to describe rainfall amounts and wind speed.

Daily temperature, vapor pressure and radiation values are represented by one cosine function in combination with a function that generates residuals. The applied method does not perform very well (Table 5). For about 60% of the grid cells the observed and generated temperatures and vapor pressure can be considered drawn from the same distribution. For global radiation this is 56%. However, one should bear in mind that the observed grid weather data have been interpolated from various meteorological stations using an automatic procedure. In the course of time many of these stations have stopped to supply data to the GTS and have been replaced by other stations. These changes are not recorded. Grid cell temperature, vapor pressure and radiation series may therefore show some sudden changes/jumps. The variance may change over time as well. Consequently, a perfect cosine form as is assumed in equation (4) cannot always be expected. Furthermore, according to Roerink et al. (2012) the CGMS global radiation values also contain irregular patterns due to the applied calculation method. Depending on the data availability, global radiation values are a mixture of measured radiation and radiation values are based on either sunshine duration, cloud cover and temperature or only on temperature.

In a next step, we tested (t-test, $p < 0.01$) for each crop if the simulated potential and rainfed yields obtained with observed grid weather and generated grid weather can considered to be drawn from the same distribution. For both simulated potential and rainfed yields this is true for more than 90% of the grid cells (Table 6). As is demonstrated in Table 5, the generated grid temperature and radiation do not always have the same distribution characteristics as the observed grid temperature and radiation and therefore the fit is not perfect. However, as the simulation results are integrated over the growing season the imperfect variance and distribution are leveled to a large extent.

4.2. Wheat yields simulation

In 1990–2008 in north-western Europe relatively cool growing seasons with sufficient solar radiation and an early start result in high simulated potential yields (Table 7). In northern Europe the growing season starts later and in the slightly warmer maritime regions the harvest is earlier, resulting in a shorter season with a lower potential yield. More to the east the growing season starts later start and the seasons are shorter leading to lower potential yields (Russia). The lowest potential yields are found on the Balkan as a result of cold winters and a relatively warm, cloudy spring.

Wheat yields are reduced by droughts during the grain filling period, i.e. the final 2 months of the growing season. In northwest and northern Europe this may occur in late summer. South of the Baltic Sea and in Western Europe the harvest is a month earlier and yields are sensitive to droughts in late spring and early summer. High rainfed yields occur along the Atlantic coast of Spain and in western Italy and western Turkey. In these regions water shortages during the growing season are limited. Due to water shortages in combination with high temperatures significantly lower yields occur in eastern Turkey, Sicily and in some regions at

Table 7
Potential dry matter yields and dry matter yield changes relative to the period 1990–2008 for the A2 and B1 emissions scenarios.

Potential yield																												
		Wheat							Maize							Sugar beet							Potato					
		A2			B1				A2			B1				A2			B1				A2			B1		
	Ref	2030	2050	2090	2030	2050	2090	Ref	2030	2050	2090	2030	2050	2090	Ref	2030	2050	2090	2030	2050	2090	Ref	2030	2050	2090	2030	2050	2090
Country	[t/ha]	%	%	%	%	%	%	[t/ha]	%	%	%	%	%	%	[t/ha]	%	%	%	%	%	%	[t/ha]	%	%	%	%	%	%
Ireland	10.6	11	18	33	9	14	16								13.7	13	29	58	14	23	31	16.0	12	18	27	10	13	13
UK	10.4	6	11	24	5	10	10	8.5	0	9	14	0	3	9	15.2	15	29	51	15	23	28	14.7	10	13	21	9	11	9
Denmark	9.7	6	13	29	4	10	14								13.8	17	35	63	19	26	37	15.0	7	10	19	6	8	8
Norway	8.5	19	27	39	17	24	24																					
Sweden	9.4	13	19	25	11	15	13								13.8	21	32	58	18	29	36	14.6	6	9	19	6	6	6
Finland	8.6	10	17	17	10	14	14																					
Estonia	8.9	8	14	14	7	11	9								10.0	0	0	12	0	0	0	7.6	6	9	9	6	6	3
Latvia	9.6	5	12	21	5	9	9								10.2	0	5	14	0	2	4	7.1	6	10	10	6	6	3
Lithuania	9.7	4	10	21	3	7	7	7.9	0	5	6	0	0	4								8.4	0	0	0	0	0	0
France	9.3	8	11	23	6	10	9	9.0	0	−3	−20	0	−3	−11	17.3	15	25	39	15	20	22	13.2	9	8	8	8	10	4
Belgium	9.2	5	8	19	3	8	8	8.4	0	0	−9	4	6	7	15.9	14	24	39	16	21	21	13.4	8	8	12	7	9	5
Netherlands	8.8	6	11	25	5	11	11	8.6	0	2	−6	4	8	10	15.5	13	24	40	16	22	24	13.7	8	8	13	8	10	6
Germany	8.6	12	16	29	11	17	17	8.9	0	2	−6	0	0	−1	16.7	13	25	40	13	19	22	13.1	6	6	6	5	5	0
Austria	8.6	11	17	28	9	13	10	9.1	−5	−10	−25	−4	−8	−15	17.4	13	23	32	14	19	19	10.0	0	0	−21	0	0	−15
Poland	8.6	8	13	25	7	11	11	9.0	−3	−6	−17	0	0	−1	15.9	13	24	40	13	19	23	8.7	0	3	3	0	0	−4
Slovakia	8.5	6	12	24	5	7	7	9.2	−5	−12	−29	−3	−9	−18	18.3	10	18	25	10	13	13	9.4	0	0	−9	0	0	−7
Czech R.	9.1	15	20	33	13	18	15	9.2	0	0	−11	0	0	0	17.1	18	32	52	18	25	28	12.4	0	0	0	0	0	−4
Hungary	7.8	4	10	20	0	4	0	9.5	−8	−21	−45	−8	−19	−35	16.0	21	32	42	17	25	16	10.2	0	−5	−21	−4	−4	−19
Romania	7.7	6	12	22	5	8	5	9.0	−6	−17	−42	−6	−16	−33	9.8	7	19	19	9	12	12	9.1	0	2	2	0	0	−6
Bulgaria	6.1	24	34	54	22	28	26	7.6	−5	−18	−47	−6	−18	−35	9.5	0	0	−26	0	−4	−19	6.9	0	−11	−40	−9	−19	−36
Slovenia	6.2	38	45	70	35	40	40	9.6	−6	−15	−37	−6	−14	−26	19.5	11	19	26	11	14	12							
Croatia	7.1	30	38	60	28	34	28	9.7	−7	−20	−43	−7	−16	−31	18.3	13	18	21	10	14	8	5.9	0	−8	−14	0	0	−11
Serbia/Mn.	6.4	31	39	61	29	35	30	9.3	−7	−19	−46	−7	−19	−36	13.0	12	16	16	8	8	4	9.5	0	−4	−17	0	−4	−17
Macedonia	5.1	44	56	82	40	48	42	8.4	−5	−18	−49	−7	−20	−39	13.7	11	11	−9	8	5	−6	9.5	0	−5	−25	0	0	−14
Albania	8.3	23	30	50	21	26	22	8.3	−4	−16	−42	−4	−14	−32	17.5	0	0	−9	0	0	−13	11.7	0	0	−6	0	0	−12
Portugal	9.8	8	11	17	7	10	5	9.7	−4	−16	−39	−3	−9	−24	18.1	9	9	9	9	13	0	12.0	10	6	−6	9	11	−4
Spain	9	12	22	38	11	18	14	8.9	−2	−10	−33	0	−4	−16	18.2	12	14	5	12	12	1	11.0	17	13	0	15	15	0
Italy	9.1	13	19	32	11	18	13	8.9	−3	−14	−39	0	−5	−19	17.2	10	10	7	9	9	−1	10.4	13	10	3	11	13	0
Greece	7.2	22	29	46	21	26	22	7.9	−4	−16	−43	−6	−17	−34	14.1	6	3	−13	0	−4	−14	10.4	8	8	3	6	6	−5
Turkey	7	20	28	48	16	23	22	8.0	0	−7	−32	−3	−11	−25	12.1	5	5	−10	0	0	−9	7.9	0	−4	−21	0	0	−12
Belorussia	8.7	0	7	16	0	4	4	8.9	0	2	−3	0	0	1	13.3	8	17	33	8	13	17	8.7	0	0	0	0	0	−4
Russia	7	0	7	16	0	6	1	8.4	−4	−13	−38	−6	−14	−29								7.8	0	3	3	0	3	−2
Moldova	8.1	0	8	12	0	0	0	8.9	−8	−19	−43	−8	−18	−34	10.0	0	8	8	0	0	−4	8.8	0	0	0	0	0	−4
Ukraine	7.7	0	7	14	0	4	0	8.9	−5	−13	−34	−6	−14	−26	11.9	11	22	29	10	16	20	8.7	0	0	0	0	0	−4
Georgia	7.3	13	20	33	10	17	14	6.8	4	4	−17	0	−3	−14	15.4	20	33	37	18	25	25							

0 not significant.

Mediterranean coast of Spain. On the Balkan summer rains are more common and rainfed yields come close to the potential level. In eastern Europe (Ukraine and Belorussia) the rainfed yields are still as high as 80% of the potential yields, rainfed yields decrease when going to the east.

In 2030, for both the A2 and B1 scenarios, the increasing CO_2 concentration results in significant potential yields increase (*t*-test, $p < 0.05$) for most countries. Rising temperatures, outside the optimal temperature range reduce the effects of increasing CO_2 concentrations in eastern Europe. In these regions yields do not increase and more to the east they decline (Fig. 1). In the period 2030–2050 potential yields increase almost everywhere. However, in the period 2050–2090 only in the A2 situation potential yields continue to increase. In the B1 situation the atmospheric CO_2 concentration increases less and the rising temperatures cause declining potential yields in southern Europe. In northern Europe only in some regions the temperature increase is less and potential yields continue to rise, elsewhere potential yields remain stable.

In 2030, for both the A2 and B1 scenarios in large areas in northern and western Europe rainfall cannot satisfy the increasing water requirements and rainfed yields do not increase. Only on the British Islands and the coastal regions of Scandinavia rainfed yields increase (Fig. 1). In eastern Europe, increasing rainfall partially compensate the effects of the increasing temperature and except for some regions in southern Ukraine and Russia rainfed yields do not change. In southern Europe enough rainfalls in winter and spring to ensure increasing rainfed yields in many regions. From 2050 to 2090 in the A2 situation gradually more rainfalls in winter and early spring and rainfed yields increase first. In the B1 situation winter and spring become drier and rainfed yields decrease in large areas in Europe. Only in some isolated areas in northern and western Europe rainfed yields continue to increase.

4.3. Maize yield simulation

Maize is a C4 crop that is planted in spring and summer. In northern Europe, the growing season is shorter resulting in lower potential yields. High potential yields occur in central Europe and the Atlantic coast of the Iberian peninsula where spring and summer are relatively dry and sunny. On the Balkan summer rains are more common and consequently the global radiation is lower resulting in lower potential yields in. In southern Europe, spring and summer temperatures are high and may fall outside the optimal temperature range, resulting in higher respiration losses and lower potential yields. High rainfed yields occur in western Europe and central eastern Europe. In southern, south eastern and eastern Europe rainfed maize yields are significantly lower due to higher temperatures and low rainfall in spring and summer. Note that rainfed yields in Albania, Greece as well as in Turkey, Spain and Portugal are very low and farmers may probably not grow this crop under rainfed conditions (Fig. 3).

In 2030 for both the A2 and B1 scenarios, on the Balkan and in south eastern Europe summer temperatures become too high and the potential yields decrease. More to the north temperature increases less and in these regions the potential yields do not change. By 2050 the increasing temperatures result in decreasing potential yields in the whole of southern Europe. In northern Europe the temperatures are lower and in various regions the rising temperatures extend the period that the crop remains in the optimum temperature range, resulting in higher potential yields. In the A2 situation the temperature continues to rise and by 2090 potential yields decline in almost every region. In the B1 situation the temperature increase is less and in the period 2050–2090 potential yields continue to decline in southern Europe while they remain constant in northern Europe. In eastern Europe the area where potential yields decline increases.

In 2030, in various southern European regions and the Balkan rainfall increases resulting in rising rainfed yields. Note that these increases are less than 0.7 ton/ha. In the A2 situation in various regions in north western Europe rainfall amounts decline and rainfed yields decline consequently. In 2050, in the A2 situation in many southern and south eastern European regions rainfed yields decline as the water availability cannot keep up with the water requirements. In the B1 scenario the situation is different, rainfed yields remain stable in the majority of regions. Only in a few isolated regions in southern Europe rainfed yields decline. However, in 2090 spring and summer become drier, the water availability cannot keep up with the water requirements and consequently rainfed yields decline almost everywhere. In the A2 situation the situation is different, the water use efficiency increases strongly as the CO_2 concentration increases resulting in stable and sometimes increasing rainfed yields in southern and south eastern Europe. Comparison with the A2 2090 results for sugar beet and potato (crops where the water use efficiency increase is less) show that these stable or rising rainfed yields can be mainly attributed to increase water use efficiency.

4.4. Sugar beet yield simulation

The optimum temperature for sugar beet is similar to the optimum temperature of the other studied C3 crops, however, at higher temperatures the CO_2 assimilation reduction is far less pronounced than for the other crops. For example, at 35 °C the assimilation is reduced to about 80% of its level at the optimum temperature (15–20 °C), whereas the wheat and potato assimilation at 35 °C are reduced to less than 1% of its level at the optimum temperature. Potential yields are highest in regions with a long sufficiently warm and sunny growing season, corresponding to the zone from Bretagne to Slovakia, the northern part of the Balkan and the Iberian peninsula (Fig. 4). To the south and southeast of this optimum zone high temperatures in summer result in high respiration losses resulting and lower potential yields. To the north, spring and summer become cooler and less sunny and potential yields decrease. More to the east (Russia) the continental influence becomes stronger and the growing season shorter, leading to lower potential yields. The rainfed sugar beet yields are highest in the humid temperate climate zone of western and central Europe, the growing season is long and the rainfall is sufficient. In the Baltic region summers are dryer and rainfed yields are lower. The lowest rainfed are found in southern Europe where summers are hot and dry (Table 8).

In 2030 in both scenarios, potential yields stagnate or decrease in some regions in southern-central Europe, northern Balkan, Turkey and the Baltic. In the Baltic region this is related to reduced radiation, in the other regions it is caused by high summer temperatures. Everywhere else the increasing temperature and CO_2 concentration result in increasing potential yields. By 2050 in south eastern Europe the summer temperature becomes too high and potential yields stagnate or decline in both scenarios. In south western Europe the temperature increase is less and the increasing CO_2 concentration compensates the negative temperature effects and potential yields stagnate. In northern Europe the rising temperatures result in higher potential yields. In 2090 in northern and western Europe the temperature remains for a longer period in the optimal temperature range than elsewhere in Europe and potential yields continue to increase in both scenarios. To the south and the east the temperature more frequently falls outside the optimal range and the potential yields decline.

In 2030 in various regions in western and central Europe, the Balkan and Turkey rainfall cannot keep up with the water requirements and rainfed yields stagnate or sometimes decline in both scenarios. Note that in the A2 scenario this situation occurs more

Table 8
Rainfed dry matter yields and dry matter yield changes relative to the period 1990–2008 for the A2 and B1 emissions scenarios.

Rainfed yield	Wheat							Maize							Sugar beet							Potato						
		A2			B1				A2			B1				A2			B1				A2			B1		
	Ref	2030	2050	2090	2030	2050	2090	Ref	2030	2050	2090	2030	2050	2090	Ref	2030	2050	2090	2030	2050	2090	Ref	2030	2050	2090	2030	2050	2090
Country	[t/ha]	%	%	%	%	%	%	[t/ha]	%	%	%	%	%	%	[t/ha]	%	%	%	%	%	%	[t/ha]	%	%	%	%	%	%
Ireland	7.9	18	18	46	15	20	20								11.8	20	30	53	19	27	27	10.8	24	18	24	18	18	6
UK	7.0	11	11	40	13	15	15	5.7	12	12	12	21	21	3	10.8	14	14	14	21	21	6	8.4	20	13	13	21	21	5
Denmark	5.0	19	19	56	15	28	28								9.8	16	21	31	20	20	20	7.4	15	7	12	15	15	2
Norway	7.3	21	31	49	19	25	31																					
Sweden	5.7	11	11	43	12	16	20								10.1	23	23	23	18	18	18	7.6	0	0	0	0	0	0
Finland	5.7	17	17	36	15	20	20																					
Estonia	6.6	14	14	27	13	18	18								8.1	0	−10	5	0	−9	−9	4.5	25	19	28	25	25	25
Latvia	7.4	15	15	37	11	18	18								8.7	0	−2	8	0	0	0	4.2	27	16	29	21	21	21
Lithuania	7.2	10	14	40	8	14	19	6.2	11	11	11	9	9	9								5.1	0	−13	−13	0	0	0
France	6.9	0	0	24	7	16	10	4.6	−10	−27	−27	0	0	−39	12.4	0	0	0	12	12	−8	7.0	0	0	0	15	18	−4
Belgium	8.2	0	3	21	0	6	6	6.9	−10	−10	−10	0	0	−12	13.9	0	5	5	13	15	5	8.6	0	0	0	0	0	−13
Netherlands	7.0	0	0	26	0	8	2	6.6	0	0	0	0	0	−16	12.7	0	0	0	12	12	1	8.6	0	0	0	0	0	−16
Germany	6.2	10	14	43	10	20	15	6.8	−7	−11	−11	0	0	−13	12.2	0	0	5	10	10	−1	7.9	0	−6	−1	0	0	−16
Austria	6.1	8	8	34	0	13	7	6.6	0	−11	−16	0	0	−21	11.0	0	−7	−7	0	0	−12	5.1	0	0	−18	0	0	−27
Poland	5.7	11	17	45	9	18	12	5.9	0	0	3	0	0	−14	11.1	9	11	16	10	10	−1	4.8	0	0	0	0	0	−15
Slovakia	5.5	13	20	53	10	20	20	4.3	0	−15	−15	0	−9	−29	10.1	10	0	0	0	−6	−18	4.5	0	−11	−11	0	0	−14
Czech R.	6.5	12	15	45	7	19	13	5.4	0	−9	−1	0	0	−18	13.2	15	15	21	14	14	3	8.0	0	−8	−8	0	0	−12
Hungary	5.1	11	18	46	0	11	4	4.7	0	−21	−27	0	−10	−42	10.7	14	6	−2	0	0	−18	4.0	0	−15	−37	0	0	−28
Romania	5.6	12	18	29	8	11	7	4.3	0	−16	−27	0	−8	−36	6.0	0	−8	−48	0	−5	−32	5.5	10	10	6	0	0	−10
Bulgaria	5.7	23	33	54	20	27	25	3.2	0	−16	−16	0	−7	−31	4.0	0	−32	−61	0	−18	−52	2.5	0	−19	−43	0	−10	−37
Slovenia	5.9	41	49	78	36	44	44	7.2	0	−7	−19	0	0	−24	15.4	16	16	7	13	18	−2							
Croatia	6.8	29	37	64	27	35	27	5.3	0	−18	−27	0	0	−32	12.3	13	−1	−12	0	0	−21	3.0	0	−7	−14	0	0	−18
Serbia/Mn.	6.0	31	40	65	28	36	30	4.1	0	−9	−17	0	−10	−44	7.2	0	−11	−23	0	−11	−28	4.7	0	−10	−24	0	0	−26
Macedonia	4.9	41	54	80	37	47	39	3.1	0	0	−9	−27	−27	−54	5.8	0	−13	−49	−24	−24	−40	4.3	0	0	−37	−27	−18	−40
Albania	6.6	22	34	54	19	29	22	1.0	0	32	−26	54	54	−11	2.1	65	103	30	98	98	21	2.8	50	50	−4	57	57	7
Portugal	4.7	0	13	13	0	15	2	0.9	0	−34	−23	0	32	−64	1.2	42	31	5	36	36	1	2.2	79	63	25	71	81	11
Spain	5.3	8	23	42	0	11	7	1.1	20	−5	−5	23	23	−34	1.8	53	53	33	58	58	23	2.3	69	59	38	64	72	34
Italy	5.1	29	37	67	26	40	33	2.5	48	29	29	46	46	−1	5.3	36	24	9	30	38	9	2.4	53	53	36	46	64	21
Greece	6.0	18	29	49	16	24	22	0.7	22	34	65	24	24	−19	3.7	0	−4	−28	0	0	−18	1.8	12	12	−8	0	6	−16
Turkey	5.4	0	11	32	0	7	7	1.1	74	58	58	55	55	21	2.0	16	−4	−35	0	−5	−31	2.1	12	12	−14	0	0	−23
Belorussia	7.0	0	4	23	0	4	4	7.1	0	0	5	0	0	0	11.0	0	0	0	0	0	−5	5.6	0	0	0	0	0	−8
Russia	4.7	0	8	33	0	13	3	2.3	38	24	24	0	21	−21								5.0	15	7	14	0	0	−8
Moldova	6.6	7	17	25	8	8	8	5.0	0	0	−14	0	−7	−27	5.5	0	0	−47	0	0	−31	5.3	0	0	0	0	0	0
Ukraine	6.1	0	6	24	0	5	−1	4.8	0	0	−15	0	0	−28	9.5	10	10	−14	0	0	−10	5.9	9	9	9	0	0	−9
Georgia	6.0	20	30	45	16	25	23	4.1	26	26	11	0	0	−25	7.5	0	0	−37	0	0	−33							

0 not significant.

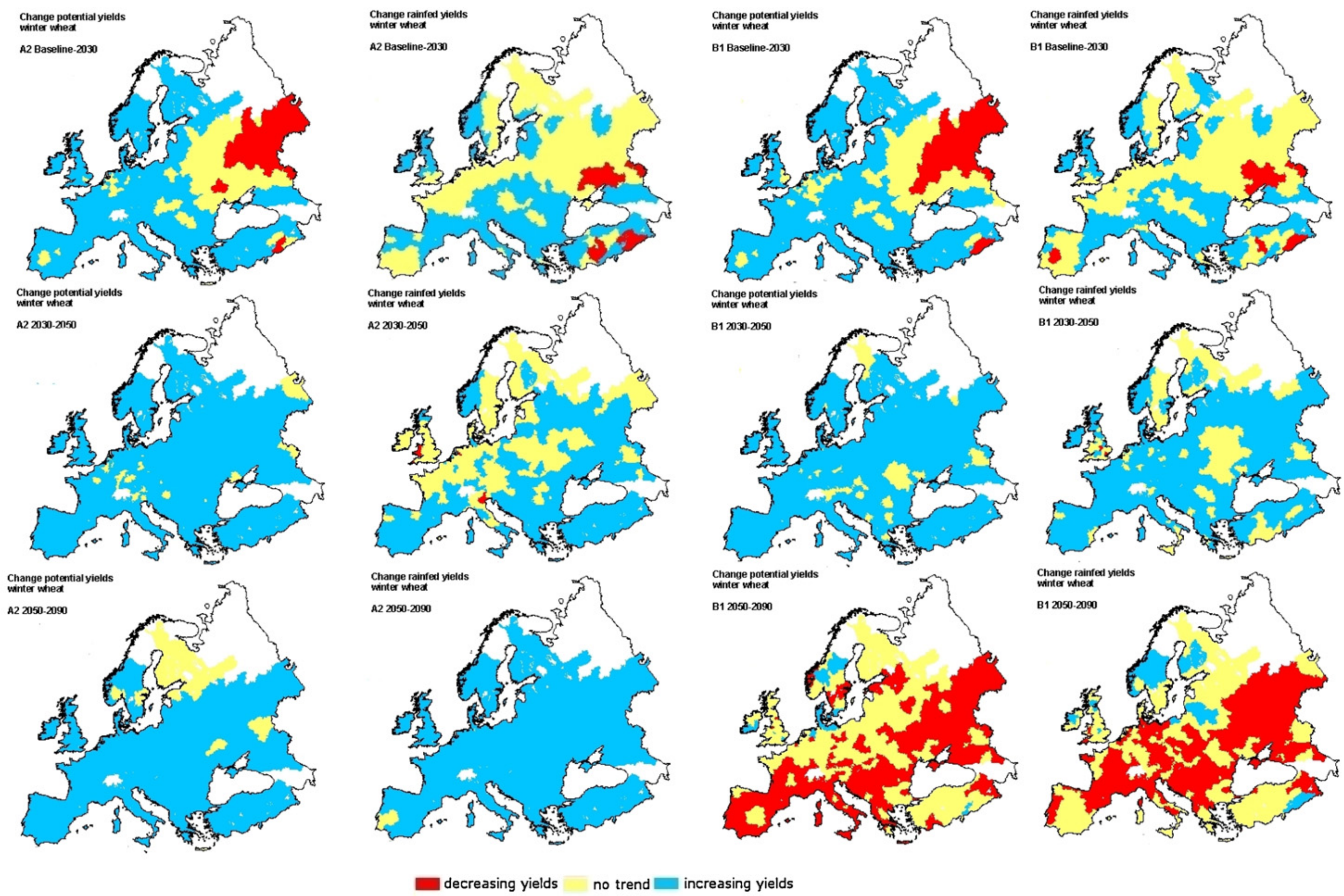

Fig. 2. Significant changes (t-test, $p = 0.05$) in potential and rainfed winter wheat yields between respectively the baseline period and 2030, 2030–2050 and 2050–2090 for the A2 and B1 emission scenarios. Baseline period is 1990–2008.

often than in the B1 situation and consequently the area where rainfed yields stagnate is larger (Fig. 3). By 2050 in southern Europe the weather becomes drier and rainfed yields decline in many regions in the A2 scenario. In the B1 scenario the drought effects are less and rainfed yields, except for some isolated regions, stagnate in many regions. In 2090 droughts intensify and the area where rainfed yields decline extends. In the A2 situation the increasing CO_2 concentration can partly compensate the drought effects in northern Europe and rainfed yields stagnate. However, in the B1 situation rainfall cannot keep up with the water requirements and rainfed yields decline almost everywhere.

4.5. Potato yield simulation

Similar to sugar beet, potatoes are planted in spring, potatoes however, are harvested earlier. Potatoes are less affected by late summer droughts and grow well under cool conditions and benefit more than sugar beets from cool springs early in the season. High potential yields occur in north western and northern Europe where the growing season is very long and relatively cool with sufficient solar radiation and rainfall. Somewhat lower yields are found in Western Europe where the growing season is warmer and shorter. To the east and on the Balkan, winters are cold and potatoes are mainly grown in summer, leading to lower potential yields. In southern Europe potatoes benefit from mild temperatures in late winter and potential yields are relatively high. The rainfed yields are highest in north western and western Europe and lower in the other regions as consequence of lower summer rainfall (Fig. 5).

In 2030 potential yields increase in northern, western and southern Europe in both scenarios (Fig. 5). In these regions the positive effects of the increasing CO_2 concentration are stronger than the negative effects of temperature increase. On the Balkan, in central and eastern Europe the increasing temperatures temper the yield increase caused by the increased CO_2 concentration. In 2050 the increasing CO_2 concentration cannot compensate the yield reduction caused by increasing temperatures in the A2 scenario. Only in northern Europe the temperatures come closer or remain for a longer period in the optimal temperature range and potential yields increase. In other regions potential yields stagnate or decrease. In the B1 scenario potential yields slightly increase in the Atlantic coastal regions of western and northern Europe as well as in Italy and Portugal (Fig. 5). Elsewhere potential yields stagnate or decrease. In 2090 potential yields continue to increase in northern and western Europe in the A2 scenario. However, the spatial distribution differs from the distribution in 2050. In southern Europe and on the Balkan the increasing temperatures intensify the potential yield decline. In the B1 scenario temperature increase dominates over the CO_2 concentration increase and the potential yields decrease in the majority of countries (Table 8).

In 2030 rainfed yields stagnate in various regions in northern and western Europe in both scenarios whereas the potential yields increase indicating that rainfall cannot sufficiently cover the water requirements. In south western Europe rainfed yields increase as the rainfall increases. In 2050 in the A2 scenario northern and central Europe becomes drier and rainfed yields stagnate or decrease in many regions (Table 8). The B1 scenario is different, droughts are less pronounced and rainfed yields continue to increase in south

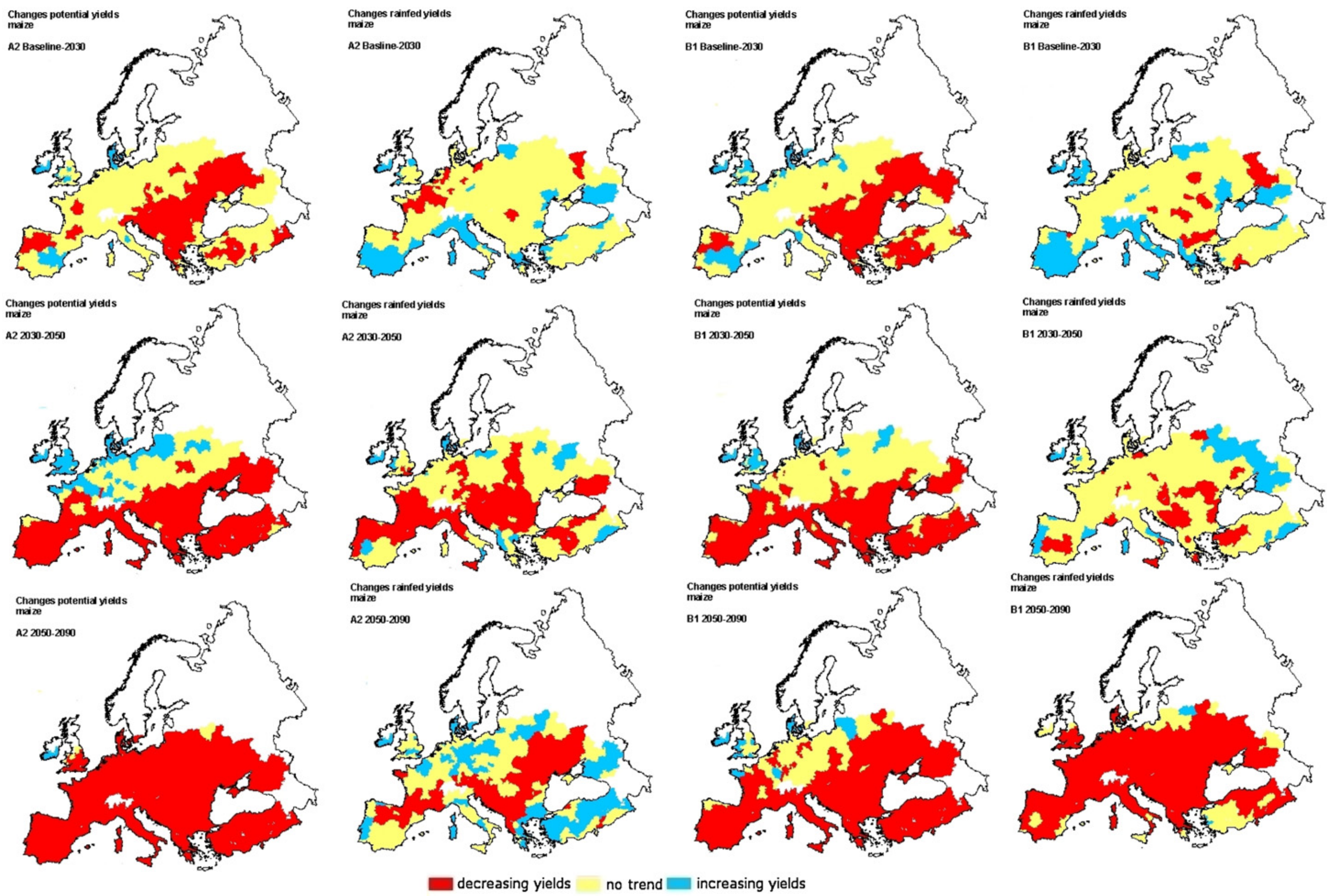

Fig. 3. Significant changes (*t*-test, $p = 0.05$) in potential and rainfed maize yields between respectively the baseline period and 2030, 2030–2050 and 2050–2090 for the A2 and B1 emission scenarios. Baseline period is 1990–2008.

western Europe. In 2090 in northern and eastern Europe after a period of decline or stagnation the increasing CO_2 concentration and increasing rainfall result in rising rainfed yields. Elsewhere rainfed yields stagnate or decrease. In the B1 scenario temperature increase dominates over the CO_2 concentration increase and rainfed yields decrease in the majority of countries. Rainfed yields decline much stronger than the potential yields indicating that the climate becomes drier in this scenario.

5. Discussion

5.1. Methodology

The method to describe daily grid cell values of temperature, vapor pressure and radiation performs not very well. However, as CGMS integrates the simulation results over space and time to obtain regional crop yields, the errors are averaged out. This indicates that the errors are more or less normally distributed. Generated grid weather values will have similar error patterns as the current grid weather and the scenario yield results have a similar quality as those obtained with current grid cell data. In theory, current weather data should follow a cosine function as described by Eq. (4). However, this is not always true and these data series are open for improvement. How this should be done falls outside the scope of this study. Grid cell data for the scenarios follow Eq. (4) correctly and may therefore be closer to reality.

Various techniques exist to correct the synthetic weather series for the correlation among grid cells (e.g. Wilks, 1998, 1999; Brissette et al., 2007). We did not apply any of these methods. In our study we generated 31 years of weather data per grid cell. Within each grid cell crop yields are simulated per intersection of administrative region and suitable soil type. The results are subsequently aggregated to sub-regional, regional and national levels. We assume that the error that occurs by omitting the correlation correction among grid cells is leveled off by the combined effect of the aggregation process, the integration over the growing season by the crop simulation model and by averaging the simulation results over the 31 years.

The area deemed suitable for a specific crop is used as weighting factor. Trends that occur on one aggregation level may be obscured on another level as a result of the aggregation process. For example, in the A2 scenario in some sub-regions in Macedonia and Greece around the year 2030 the rainfed sugar beet yields begin to decline (Fig. 4). In the surrounding sub-regions this decline is not yet visible and on a national level it disappears (Table 8).

To generate synthetic rainfall series we used the same rainfall occurrence patterns as in the baseline situation. As the climate becomes drier the number of dry days increase. The precipitation amounts are thus distributed over a smaller number of rainfall occurrences, whereas the dry spells may be longer than assumed. The simulated rainfed yields may be overestimated in the areas where the climate becomes drier. As the number of wet days may be under-estimated both the temperature and the radiation are under-estimated as well. In areas where the ambient temperature is lower than the optimum temperature potential yields may be under-estimated, however in those areas where the ambient temperature is higher than the optimum, the under-estimation is less.

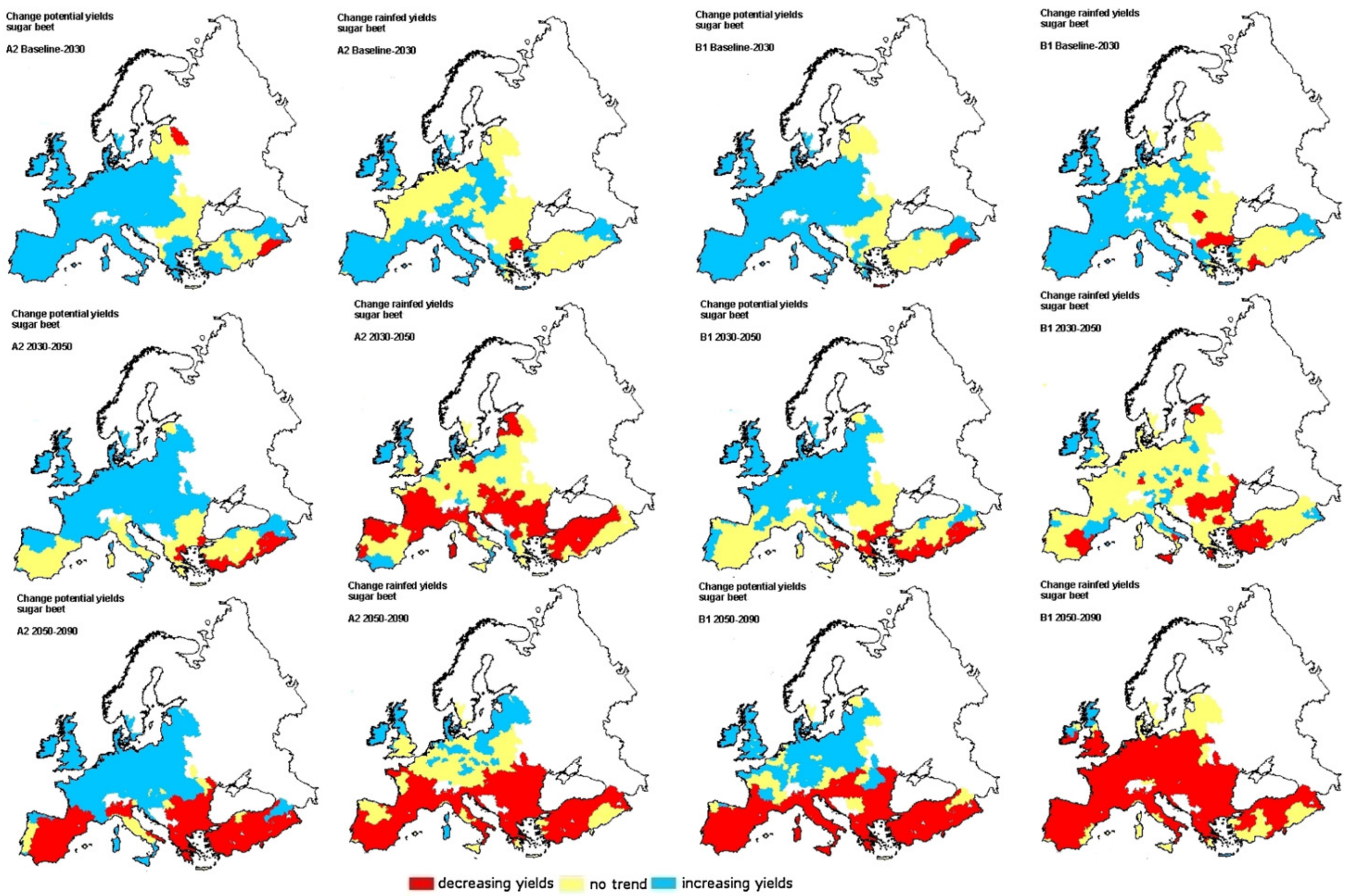

Fig. 4. Significant changes (*t*-test, $p = 0.05$) in potential and rainfed sugar beet yields between respectively the baseline period and 2030, 2030–2050 and 2050–2090 for the A2 and B1 emission scenarios. Baseline period is 1990–2008.

The modeled CO_2 influence on crop growth is based on studies that consider a doubling of the CO_2 concentration (Section 3.2.1). However the A2 CO_2 concentration in 2090 is 771 ppm which is more than the double. We linearly extrapolated the crop parameters in Table 2 to the CO_2 level of 2090. However, there is no scientific evidence that this assumption is correct.

5.2. Simulation results

5.2.1. Transpiration

The increasing CO_2 concentration reduces crop transpiration (e.g. Wand et al., 1999) and boosts crop assimilation. Less water is needed for the same dry matter amount. Increasing rainfed yields, as found in our results, can be attributed to increase rainfall, a higher water use efficiency or a combination of both. As time progresses, stagnating rainfed yields indicate that the climate becomes drier. For the C3 crops this effect is smaller than for C4 crops as a result of different reduction rates. The transpiration reduction rate for C3 crops is small, it is 10% at the end of the century. For C4 crops (maize) it is much higher, 26%.

As the climate changes, land suitability changes as well (e.g. Daccache et al., 2012). This has repercussions on the spatial crop distribution. As rainfall will decrease and possibilities for irrigation become less, the less productive soils may be taken out of production. For the future scenarios we used land use information of the year 2008. As consequence, the aggregation process (Eq. (1)) will put too much weight on the future unsuitable soils and the regional rainfed crop yields may therefore be under estimated in scenario calculations.

5.2.2. Wheat

New varieties and improved management have nearly tripled wheat yields in Europe between 1961 and today (Ewert et al., 2005). The contribution of increased CO_2 concentration to these yields increase is limited, less than 4% (Ewert et al., 2007). Supit et al. (2010b) reported that the actual wheat yield trend slowed down in the period 1976–2005 in some European regions. This could be the result of increasing winter and spring temperatures which lead to a shorter growing season. This study shows that the climatic potential for winter wheat for both potential and rainfed situations continue to rise from the present to 2050 (Fig. 2). After 2050, depending on the CO_2 concentration and temperature rise, potential as well as rainfed yields continue to increase (A2 scenario) or stagnate and ultimately decline (B1 scenario). However in many regions the maximum possible yields are not obtained (Supit et al., 2010b) and there is still room for yield improvement as new breeding techniques, improved varieties with an improved light and nitrogen efficiencies (Loomis and Amthor, 1999; Borlaug, 2000), improved pest management techniques become available. Wheat yields may continue to increase even if the climatic potential after 2050 declines.

Assuming that winter wheat represents the C3 crops planted in autumn and winter we can speculate that these crops may profit from climate change up to 2050. After 2050, improved crop

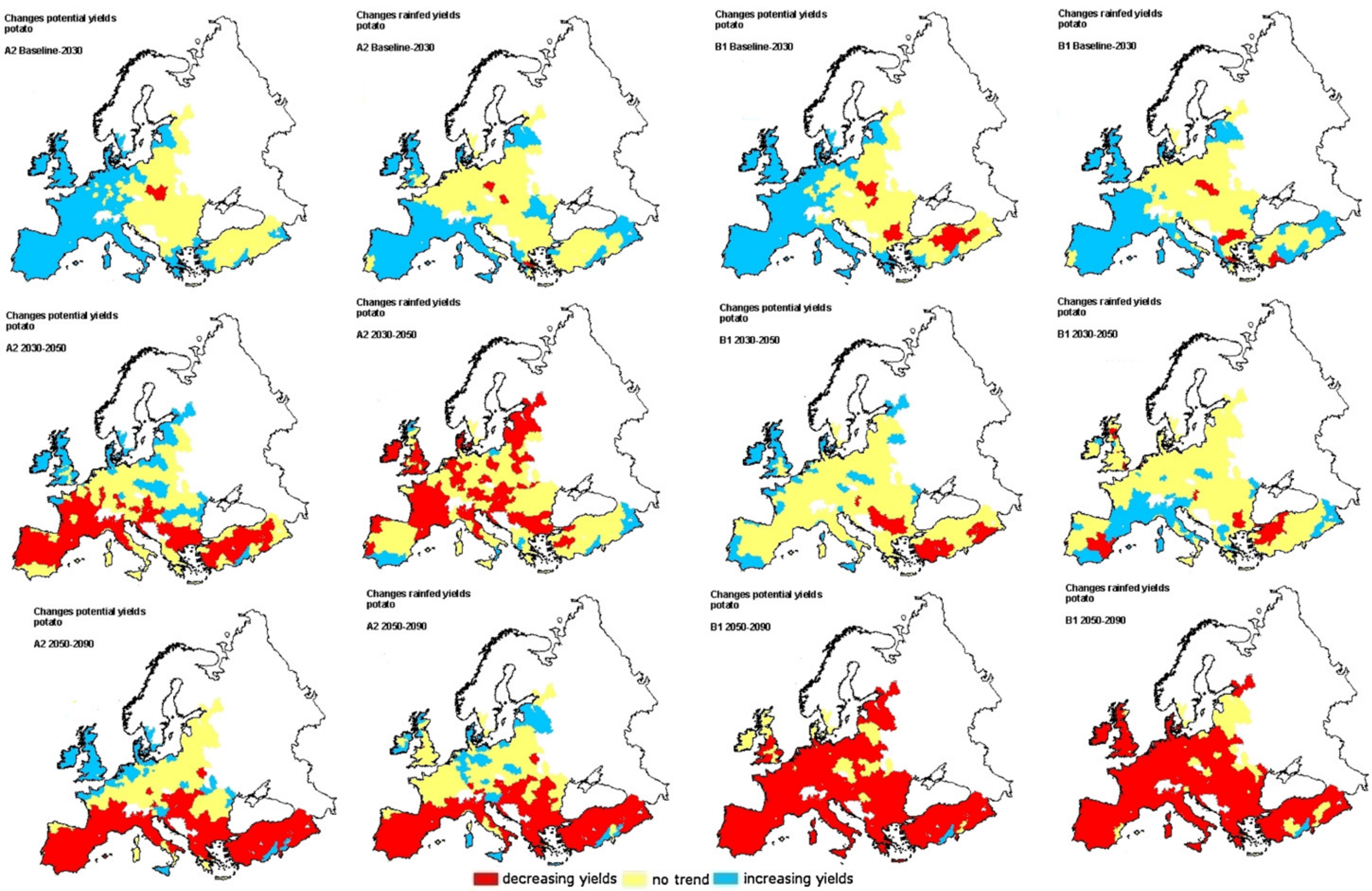

Fig. 5. Significant changes (*t*-test, $p = 0.05$) in potential and rainfed potato yields between respectively the baseline period and 2030, 2030–2050 and 2050–2090 for the A2 and B1 emission scenarios. Baseline period is 1990–2008.

management techniques, improved varieties, etc. may also contribute to increasing yields in many regions.

5.2.3. Maize

By the end of the century the climatic potential for maize decreases as temperature increases in southern Europe (Fig. 3). We used the same planting dates as in the present situation. In reality however, maize will be planted earlier in the season to avoid droughts and extreme temperatures in summer. The climatic potential for maize cultivation may therefore decrease less as is estimated. However, especially in southern Europe, droughts cannot always be avoided and rainfed maize cultivation may not be feasible anymore. Unless irrigation is possible, it may probably be abandoned. Future maize production in southern Europe depends on irrigation water availability and thus on the willingness of policy makers to redirect the available water to the agricultural sector. Similar to maize, other summer crops in southern Europe may also experience water shortages. In general, by the end of the century summer crop cultivation in southern Europe depend on the competition between various water consuming sectors. Probably the less productive soils will be taken out of production.

Maize production may shift to the north, to the temperate climate zones where presently the growing season is too short. In these regions maize is mainly cultivated for fodder (e.g. Netherlands and Denmark). By the end of the century the climatic conditions improve and grain maize cultivation may increase. The occurring summer droughts may make supplementary irrigation necessary.

5.2.4. Sugar beet and potato

Sugar beet and potato are C3 crops planted in spring. The difference between actual yields and what is potentially possible is about 20–30 ton/ha for all countries (Supit et al., 2010b). There is certainly room for yield improvement and actual yields may continue to increase in the future. In the A2 situation this process, especially in northern Europe, may continue much longer than in the B1 situation where the limited CO_2 concentration increase will negate the yield research advances in an earlier stage (Fig. 4). Potato is more susceptible to high temperatures than sugar beets and high temperatures will temper the increasing yields earlier than for sugar beet (Fig. 5).

Similar to maize, we used the same planting dates as in the present situation. In reality however, as the spring temperatures rise, planting may start earlier, the growing season will thus extend and consequently yields may increase provided enough water is available. In southern Europe however, by the end of the century temperatures in late spring and summer become too high and in combination with the occurring droughts crop yields decline and irrigation will be necessary to maintain the production level. Competition between various water using sectors will decide the distribution and amount of available water. Rainfed potato and sugar beet cultivation will gradually disappear and irrigated production may probably be limited to those areas where enough water is available. The main production centers remain in northern Europe.

6. Conclusion

This study only considers climate change effects on various crops. Further research should address how adaptation strategies such changing planting dates, other crop varieties etc., affect crop yield. Up to 2050, regardless of the followed scenario winter wheat and crops planted in autumn and winter in general, may benefit from the increasing temperature and CO_2 concentration. After 2050 yield development depends on further development of the temperature and CO_2 concentration increase.

Maize and probably other C4 crops planted in summer may initially benefit from the increasing CO_2 concentration as the water use efficiency increases. However by the end of the century in southern Europe, unless irrigation is applied, rising temperatures and water shortages may cause declining yields to a point that crop production is not feasible anymore. In the temperate climate zone in northern, western and part of central Europe the increasing temperature may have a positive effect on crop yield and production may increase. Due to summer droughts supplementary irrigation may be necessary in these regions.

Root crops planted in spring (sugar beets, potato) may initially benefit from the increasing CO_2 concentration and temperature. After 2030 in southern Europe, depending on the crop type, potential yields stagnate and in the course of time decline. In northern and western Europe potential yields may continue to increase until the end of the century. Potato is more susceptible to high temperatures and potential yields decrease earlier than sugar beets and may decline also in northern Europe. As less rainfalls in spring and summer, rainfed potato and sugar beet yields initially stagnate and in the course of time decline, first in the south, gradually extending to the north. Irrigation may be necessary.

In summary, climate change impacts depend on species and region: autumn and winter crops may benefit from the changing climate. Spring and summer crops initially may benefit from the changing climate as well, however in the course of time yields decline, first in the south and later also in the north. To maintain a stable yield level, irrigation is required in southern Europe. In northern Europe supplementary irrigation is needed in summer. Adaptation strategies such as changes in farm planning and developing new breeding lines should take these regional differences into account.

Acknowledgments

This research was executed in the framework of the SCENES project (http://www.environment.fi/syke/scenes) funded by the EU 6th Framework Programme. We like to thank the MARS Unit of the Institute for Environment and Sustainability of the Joint Research Centre of the European Commission, Ispra, Italy for providing data from the MARS Crop Growth Monitoring System and its related databases.

Appendix A. Supplementary data

Supplementary data associated with this article can be found, in the online version, at http://dx.doi.org/10.1016/j.agrformet.2012.05.005.

References

Alcamo, J., Flörke, M., Märker, M., 2007. Future long-term changes in global water resources driven by socio-economic and climatic changes. Hydrol. Sci. J. 52, 247–275.

Allen, S.G., Idso, S.B., Kimball, B.A., Baker, J.T., Allen, L.H., Mauney, J.R., Radin, J.W., Anderson, M.G., 1990. Effects of air temperature on atmospheric CO2-plant growth relationships. Report TR048. U.S. Dep. of Energy/U.S. Dep. of Agriculture, Washington DC, USA.

Amthor, J.S., 2001. Effects of atmospheric CO_2 concentration on wheat yield: review of results from experiments using various approaches to control CO_2 concentration. Field Crops Res. 73, 1–34.

Asseng, S., Jamieson, P.D., Kimball, B., Pinter, P., Sayre, K., Bowden, J.W., Howden, S.M., 2004. Simulated wheat growth affected by rising temperature, increased water deficit and elevated atmospheric CO_2. Field Crops Res. 85, 85–102.

Barrow, E.M., Semenov, M.A., 1995. Climate change scenarios with high spatial and temporal resolution for agricultural applications. Forestry 68, 349–360.

Battisti, D.S., Naylor, R.L., 2009. Historical warnings of future food insecurity with unprecedented seasonal heat. Science 323, 240–244.

Beek, E.G., Stein, A., Jansen, L.L.F., 1992. Spatial variability and interpolation of daily precipitation amount. Stochastic Hydrol. Hydraul. 6, 304–320.

Bignon, J., 1990. Agrométéorologie et physiologie du maïs grain dans la communauté Européenne. Publication EUR 13041 FR of the Office for Official Publications of the EU, Luxembourg.

Boogaard, H.L., van Diepen, C.A., Rötter, R.P., Cabrera, J.M.C.A., van Laar, H.H., 1998. WOFOST 7.1; user's guide for the WOFOST 7.1 crop growth simulation model and WOFOST Control Center 1.5. Wageningen, SC-DLO, 1998. Techn. Doc. 52, 144.

Boons-Prins, E.R., Koning, G.H.J., van de Diepen, C.A., Penning de Vries, F.W.T., 1993. Crop-specific parameters for yield forecasting across the European Communtiy. Simulation Reports CABO-TT, no 32. Wageningen, The Netherlands.

Borlaug, N.E., 2000. Ending world hunger. The promise of biotechnology and the threat of antiscience zealotry. Plant Physiol. 124, 487–490.

Brissette, F.P., Khalili, M., Leconte, R., 2007. Efficient stochastic generation of multi-site synthetic precipitation data. J. Hydrol. 345, 121–133.

Brown, R.A., Rosenberg, N.J., 1997. Sensitivity of crop yield and water use to change in a range of climatic factors and CO_2 concentrations: a simulation study applying EPIC to the central USA. Agricult. Forest Meteorol. 83, 171–203.

Buishand, T.A., 1978. Some remarks on the use of daily rainfall models. J. Hydrol. 36, 295–308.

Burton, T., Sharpe, D., Jenkins, N., Bossanyi, E., 2001. Wind Energy Handbook, 1st ed. Wiley, New York.

Carta, J.A., Ramírez, P., 2007. Analysis of two-component mixture Weibull statistics for estimation of wind speed distributions. Renew. Energy 32, 518–531.

Carbonneau, A., Riou, C., Guyon, D., Riom, J., Schneider, C., 1992. Agrométéorologie de la vigne en France. Publication EUR 13911 FR of the Office for Official Publications of the EU, Luxembourg.

Chapman, T.G., 1997. Stochastic models for daily rainfall in the Western Pacific. Math. Comput. Simulat. 43, 351–358.

Chapman, T.G., 1998. Stochastic modelling of daily rainfall: the impact of adjoining wet days on the distribution of rainfall amounts. Environ. Model. Software 13, 317–324.

Chen, J., 1984. Uncoupled multi-layer model for the transfer of sensible and latent heat flux densities from vegetation. Boundary Layer Meteorol. 28, 213–226.

Cure, J.D., 1985. Carbon dioxide doubling responses: a crop survey. In: Strain, B.R., Cure, J.D. (Eds.), Direct Effects of Increasing Carbon Dioxide on Vegetation. DOE/ER-0238. U.S. Dep. of Energy, Washington D.C., USA, pp. 99–116.

Cure, J.D., Acock, B., 1986. Crop responses to carbon dioxide doubling; a literature survey. Agricult. Forest Meteorol. 38, 127–145.

Daccache, A., Keay, C., Jones, R.J.A., Weatherhead, K., Stalham, M.A., Knox, J.W., 2012. Climate change and land suitability for potato production in England and Wales: impacts and adaptation. J. Agricult. Sci. 150, 161–177.

Diepen, C.A. van, Rappoldt, C., Wolf, J., Keulen, H. van, 1988. Crop growth simulation model WOFOST. Documentation version 4.1. In: Centre for World Food Studies. Wageningen, The Netherlands.

De Temmerman, L., Wolf, J., Colls, J., Bindi, M., Fangmeier, A., Finnan, J., Ojanpera, K., Pleijel, H., 2002. Effect of climatic conditions on tuber yield (*Solanum tuberosum* L.) in the European 'CHIP' experiments. Eur. J. Agron. 17, 243–255.

van Diepen, C.A., van der Wal, T., 1995. Crop growth monitoring and yield forecasting at regional and national scale. In: Dallemand, J.F., Vossen, P. (Eds.), Agrometeorological Models: Theory and Applications. Publication EUR16008 FR of the Office for Official Publications of the EU, Luxembourg.

van Diepen, C.A., Wolf, J., van Keulen, H., 1989. WOFOST: a simulation model of crop production. Soil Use Manage. 5, 16–24.

Dufresne, 2007a. ENSEMBLES IPSL-CM4 SRESA2 run1, daily values. World Data Center for Climate. CERA-DB ENSEMBLES_IPCM4_SRA2_1_D. http://cera-www.dkrz.de/WDCC/ui/Compact.jsp?acronym=ENSEMBLES_IPCM4_SRA2_1_D.

Dufresne, 2007b. ENSEMBLES IPSL-CM4 SRESB1 run1, daily values. World Data Center for Climate. CERA-DB ENSEMBLES_IPCM4_SRB1_1_D. http://cera-www.dkrz.de/WDCC/ui/Compact.jsp?acronym=ENSEMBLES_IPCM4_SRB1_1_D.

Dufresne, 2007c. ENSEMBLES IPSL-CM4 20C3M run1, daily values. World Data Center for Climate. CERA-DB "ENSEMBLES_IPCM4_20C3M_1_D". http://cera-www.dkrz.de/WDCC/ui/Compact.jsp?acronym=ENSEMBLES_IPCM4_20C3M_1_D.

Easterling, W.E., Mearns, L.O., Hays, C.J., Marx, D., 2001. Comparison of agricultural impacts of climate change calculated from high and low resolution climate change scenarios. Part II. Accounting for adaptation and CO_2 direct effects. Climate Change 51, 173–197.

Ewert, F., Rounsevell, M.D.A., Reginster, I., Metzger, M.J., Leemans, R., 2005. Future scenarios of European agricultural land use I. Estimating changes in crop productivity. Agricult. Ecosyst. Environ. 107, 101–116.

Ewert, F., Porter, J.R., Rounsevell, 2007. Crop Models CO_2, and Climate Change. Science 315, 459.

Falisse, A., 1992. Aspects agrométéorologiques du dévelopment des cultures ans le Benelux et les régions voisines. In: Etude pour la betterave sucrière, le colza, le pois, le froment et l'avoine. Publication EUR 13910 FR of the Office for Official Publications of the EU, Luxembourg.

Falisse, A., Decelle, Y., 1990. Froment, Avoine; Etude effectuée par la faculté des sciences Agronomiques de Gembloux (Belgique). Projet pilote de télédétection appliquée aux statistique agricoles. Ispra, Italy.

Foufoula-Georgiou, E., Lettenmaier, D.P., 1987. A Markov renewal model for rainfall occurrences. Water Resour. Res. 23, 875–884.

Franzaring, J., Högy, P., Fangmeier, A., 2008. Effects of free-air CO_2 enrichment on the growth of summer oilseed rape (*Brassica napus* cv. Campino). Agricult. Ecosyst. Environ. 128, 127–134.

Giannakopoulos, C., Le Sager, P., Bindi, M., Moriondo Kostopoulou, E., Goodess, C.M., 2009. Climatic changes and associated impacts in the Mediterranean resulting from global warming. Global Planet Change 68, 209–224.

Giorgi, F., Bi, X., 2005. Updated regional precipitation and temperature changes for the 21st century from ensembles of recent AOGCM simulations. Geophys. Res. Lett. 32, 4, http://dx.doi.org/10.1029/2005GL024288.

Gisat, 2003. Studies in support to the MARS project. Crop Monographies on Candidate Countries. MOCA Study. Final report. Contract No: 20363-2002-12 F1ED ISP CZ.

Goudriaan, J., 1977. Crop micrometeorology: a simulation study. In: Simulation Monographs. Pudoc, Wageningen, Netherlands.

Goudriaan, J., 1990. Primary productivity and CO_2. In: Goudriaan, J., van Keulen, H., van Laar, H.H. (Eds.), The Greenhouse Effect and Primary Productivity in European Agro-Ecosystems. Pudoc, Wageningen, Netherlands, pp. 23–25.

Goudriaan, J., Laar, H.H., van Keulen, H., van Louwerse, W., 1984. Simulation of the effect of increased atmospheric CO_2 on assimilation and transpiration of a closed crop canopy. Wissenschaftliche Zeitschrift der Humboldt-Universität zu Berlin. Math. Nat. R.33, 352–356.

Goudriaan, J., Laar, H.H., van Keulen, H., van Louwerse, W., 1985. Photosynthesis, CO_2 and plant production. In: Day, W., Atkins, R.K. (Eds.), Wheat Growth and Modelling. NATO ASI Series. Serie A: Life Sciences, Vol. 86. Plenum Publishing, New York, USA, pp. 107–122.

Goudriaan, J., de Ruiter, H.E., 1983. Plant growth in response to CO_2 enrichment, at two levels of nitrogen and phosphorus supply. 1. Dry matter, leaf area and development. Neth. J. Agricult. Sci. 31, 157–169.

Goudriaan, J., Unsworth, M.H., 1990. Implications of increasing carbon dioxide and climate change for agricultural productivity and water resources. In: Impact of Carbon Dioxide, Trace Gasses, and Climate Change on Global Agriculture. ASA Special Publication no. 53. American Society of Agronomy, Crop Science Society of America, and Soil Science Society of America, Madison, USA, pp. 111–130.

Graham, L.P., Hagemann, S., Jaun, S., Beniston, M., 2007. On interpreting hydrological change from regional climate models. Clim. Change 81, 97–122, http://dx.doi.org/10.1007/s10584-006-9217-0.

Hagemann, S., Chen, C., Haerter, J.O., Heinke, J., Gerten, D., Piani, C., 2011. Impact of a statistical bias correction on the projected hydrological changes obtained from three GCMs and two hydrology models. J. Hydrometeorol. 12, 556–578, http://dx.doi.org/10.1175/2011JHM1336.1.

Hough, M.N., 1990. Agrometeorological aspects of crops in the United Kingdom and Ireland. In: A Review for Sugar Beet, Oilseed Rape, Peas, Wheat, Barley, Oats, Potatoes, Apples and Pears. Publication EUR 13039 EN of the Office for Official Publications of the EU, Luxembourg.

Idso, S.B., 1990. Interactive effects of carbon dioxide and climate variables on plant growth. In: Impact of Carbon Dioxide, Trace Gasses, and Climate Change on Global Agriculture. ASA Special Publication no. 53. American Society of Agronomy, Crop Science Society of America, and Soil Science Society of America, Madison, USA, pp. 61–69.

Ines, A.V.M., Hansen, J.W., 2006. Bias correction of GCM rainfall for crop simulation studies. Agricult. Forest Meteorol. 138, 44–53.

INRA, 1995. Users' Guide for the Elaboration of the European Soil Database, Version 3.1. INRA publication, Orléans, pp. 16.

Jaramillo, O.A., Borja, M.A., 2004. Wind speed analysis in La Ventosa, Mexico: a bimodal probability distribution case. Renew. Energy 29, 1613–1630.

Jones, R.J.A., Buckley, B., 1996. European soil database. In: Information Access and Data Distribution Procedures. EUR 17266 EN, Space Applications Institute, Joint Research Centre of the European Commission, Ispra, Italy, pp. 35.

Katz, R.W., 1977. Precipitation as chain dependent process. J. Appl. Meteorol. 16, 308–671.

van Keulen, H., Wolf, J. (Eds.), 1986. Modelling of Agricultural Production: Weather, Soils and Crops. Simulation Monographs. Pudoc, Wageningen, The Netherlands.

Kimball, B.A., 1983. Carbon dioxide and agricultural yield: an assemblage and analysis of 430 prior observations. Agron. J. 75, 779–788.

Lazar, C., Genovese, G. (Eds.), 2004. Methodology of the MARS Crop Yield Forecasting System. Volume 2. Agrometeorological Data Collection, Processing and Analysis. European Communities (ISBN 92-894-8181-1).

Le Bas, C., 1996. Base de données géographique des sols d'Europe. Version 3.1ß. EUR 16380 FR, Space Applications Institute, Joint Research Centre of the European Commission, Ispra, Italy, pp. 39.

Lobell, D.B., Field, C.B., 2007. Global scale climate—crop yield relationships and the impacts of recent warming. Environ. Res. Lett. 2, 014002.

Loomis, R.S., Amthor, J.S., 1999. Yield potential, plant assimilatory capacity, and metabolic efficiencies. Crop Sci. 39, 1584–1596.

Long, S.P., Ainsworth, E.A., Leakey, A.D.B., Nosberger, J., Ort, D.R., 2006. Food for thought: lower than expected crop yield stimulation with rising CO_2 concentrations. Science 312, 1918–1921.

Matalas, N.C., 1967. Mathematical assessment of synthetic hydrology. Water Resour. Res. 3, 937–945.

Meehl, G.A., Covey, C., Delworth, T., Latif, M., McAvaney, B., Mitchell, J.F.B., Stouffer, R.J., Taylor, K.E., 2007. The WCRP CMIP3 multi-model dataset: a new era in climate change research. Bull. Am. Meteorol. Soc. 88, 1383–1394.

Micale, F., Genovese, G., 2004. Methodology of the MARS Crop Yield Forecasting System. Vol. 1. Meteorological Data Collection, Processing and Analysis, Publication EUR 21291 EN of the Office for Official Publications of the EU, Luxembourg.

Miglietta, F., Magliulo, V., Bindi, M., Cerio, L., Vaccari, F.P., Loduca, V., Peressotti, A., 1998. Free air CO_2 enrichment of potato (*Solanum tuberosum* L.): development, growth and yield. Global Change Biol. 4, 163–172.

Moriondo, M., Giannakopoulos, C., Bindi, M., 2010. Climate change impact assessment: the role of climate extremes in crop yield simulation. Climate Change, http://dx.doi.org/10.1007/s10584-010-9871-0.

Nakićenović, N., Davidson, O., Davis, G., Grübler, A., Kram, T., Rovere, E.L.L., Metz, B., Morita, T., Pepper, W., Pitcher, H., Sankovski, A., Shukla, P., Swart, R., Watson, R., Dadi, Z., 2000. Emissions Scenarios—Summary for Policymakers. Intergovernmental Panel on Climate Change, Geneva.

Narciso, G., Ragni, P., Venturi, A., 1992. Agrometeorological aspects of crops in Italy, Spain and Greece. In: A Summary Review for Common and Durum Wheat, Barley, Maize, Rice, Sugar Beet, Sunflower, Soya Bean, Rape, Potato, Cotton, Olive and Grape Crops. Publication EUR 14124 EN of the Office for Official Publications of the EU, Luxembourg.

New, M., Hulme, M., Jones, P., 2000. Representing twentieth-century space–time climate variability. Part II: development of 1901–96 monthly grids of terrestrial surface climate. J. Climate 13, 2217–2238.

Nozawa, 2005a. IPCC DDC AR4 CCSR-MIROC3.2_(med-res) SRESA2 run1. World Data Center for Climate. CERA-DB "MIROC3.2_mr_SRESA2_1". http://cera-www.dkrz.de/WDCC/ui/Compact.jsp?acronym=MIROC3.2_mr_SRESA2_1.

Nozawa, 2005b. IPCC DDC AR4 CCSR-MIROC3.2_(med-res) SRESB1 run1. World Data Center for Climate. CERA-DB "MIROC3.2_mr_SRESB1_1". http://cera-www.dkrz.de/WDCC/ui/Compact.jsp?acronym=MIROC3.2_mr_SRESB1_1.

Nozawa, 2005c. IPCC DDC AR4 CCSR-MIROC3.2_(med-res) 20C3M run1. World Data Center for Climate. CERA-DB "MIROC3.2_mr_20C3M_1". http://cera-www.dkrz.de/WDCC/ui/Compact.jsp?acronym=MIROC3.2_mr_20C3M_1.

NRC, 2003. Understanding climate change feedbacks. Report of the Panel on Climate Change Feedbacks, National Research Council. National Academies Press, Washington, 166 pp.

Parry, M.L., Rosenzweig, C., Iglesias, A., Livermore, M., Fischer, G., 2004. Effects of climate change on global food production under SRES emissions and socioconomic scenarios. Global Environ. Change 14, 53–67.

Penning de Vries, F.W.T., Jansen, D.M., ten Berge, H.F.M., Bakema, A., 1989. Simulation of ecophysiological processes of growth in several annual crops. In: Simulation Monographs 29. Pudoc, Wageningen.

Piani, C., Haerter, J.O., Coppola, E., 2009. Statistical bias correction for daily precipitation in regional climate models over Europe. Theor. Appl. Climatol. 99, 187–192, http://dx.doi.org/10.1007/s00704-009-0134-9.

Qaderi, M.M., Reid, D.M., 2005. Growth and physiological responses of canola (*Brassica napus*) to UV-B and CO_2 under controlled environment conditions. Physiologia Plantarum 125, 247–259.

Racsko, P., Szeidl, L., Semenov, M., 1991. A serial approach to local stochastic weather models. Ecol. Model. 57, 27–41.

Ramírez, P., Carta, J.A., 2006. The use of wind probability distributions derived from the maximum entropy principle in the analysis of wind energy. A case study. Energy Convers. Manage. 47, 2564–2577.

Richardson, C.W., 1981. Stochastic simulation of daily precipitation, temperature, and solar radiation. Water Resour. Res. 17, 182–190.

Roeckner, 2005. IPCC DDC AR4 ECHAM5/MPI-OM SRESA2 run1. World Data Center for Climate. CERA-DB "EH5_MPI_OM_SRESA2_1". http://cera-www.dkrz.de/WDCC/ui/Compact.jsp?acronym=EH5_MPI_OM_SRESA2_1.

Roeckner, 2006. ENSEMBLES ECHAM5-MPI-OM SRESB1 run1, daily values. World Data Center for Climate. CERA-DB "ENSEMBLES_MPEH5_SRB1_1_D". http://cera-ww.dkrz.de/WDCC/ui/Compact.jsp?acronym=ENSEMBLES_MPEH5_SRB1_1_D.

Roeckner, 2007. ENSEMBLES ECHAM5-MPI-OM 20C3M run1, daily values. World Data Center for Climate. CERA-DB "ENSEMBLES_MPEH5_20C3M_1_D". http://cera-www.dkrz.de/WDCC/ui/Compact.jsp?acronym=ENSEMBLES_MPEH5_20C3M_1_D.

Roerink, G.J., Bojanowski, J., De Wit, A.J.W., Eerens, H., Supit, I., Leo, O., Boogaard, H.L., 2012. Evaluation of MSG-derived global radiation estimates for application in a regional crop model. Agricult. Forest Meteorol. 160, 36–47.

Russell, G., Wilson, G.W., 1994. An Agro-Pedo-Climatological Knowledge Base of Wheat in Europe. Publication EUR 15789 EN of the Office for Official Publications of the EU, Luxembourg.

Russell, G., 1990. Barley Knowledge Base. Publication EUR 13040 EN of the Office for Official Publications of the EU, Luxembourg.

Semenov, M.A., Barrow, E.M., 1997. Use of a stochastic weather generator in the development of climate change scenarios. Climatic Change 35, 397–414.

Semenov, M.A., Brooks, R.J., Barrow, E.M., Richardson, C.W., 1998. Comparison of the WGEN and LARS-WG stochastic weather generators in diverse climates. Climate Res. 10, 95–107.

Semenov, M.A., Brooks, R.J., 1999. Spatial interpolation of the LARS-WG stochastic weather generator in Great Britain. Climate Res. 11, 137–148.

Semenov, M.A., 2007. Development of high-resolution UKCIP02-based climate change scenarios in the UK. Agricult. Forest Meteorol. 144, 127–138.
Semenov, M.A., Stratonovitch, P., 2010. Use of multi-model ensembles from global climate models for assessment of climate change impacts. Climate Res. 41, 1–14.
Sharda, V.N., Das, P.K., 2005. Modelling weekly rainfall data for crop planning in a sub-humid climate of India. Agricult. Water Manage. 76, 120–138.
Sheffield, J., Wood, E.F., 2007. Projected changes in drought occurrence under future global warming from multi-model, multi-scenario, IPCC AR4 simulations. Climate Dyn. 31, 79–105, http://dx.doi.org/10.1007/s00382-007-0340-z.
Solomon, S., Qin, D., Manning, M., Chen, Z., Marquis, M., Averyt, K., Tignor, M.M.B., Miller, H.L. (Eds.), 2007. Climate Change 2007: The Physical Science Basis. Contribution of Working Group I to the Fourth Assessment Report of the Intergovernmental Panel on Climate Change. Cambridge University Press, Cambridge, UK.
Stern, R.D., Coe, R., 1984. A model fitting analysis of daily rainfall data. J. R. Stat. Soc. A147, 1–34.
Suhaila, J., Jemian, A.A., 2007. Fitting daily rainfall amount in peninsular Malaysia using several types of exponential distributions. J. Appl. Sci. Res. 3, 1027–1036.
Supit, I., Van Diepen, C.A., Boogaard, H.L., Ludwig, F., Baruth, B., 2010a. Trend analysis of the water requirements, consumption and deficit of field crops in Europe. Agricult. Forest Meteorol. 150, 77–78.
Supit, I., Van Diepen, C.A., De Wit, A.J.W., Kabat, P., Baruth, B., Ludwig, F., 2010b. Recent changes in the climatic yield potential of various crops in Europe. Agricult. Syst. 103, 683–694.
Supit, I., Hooijer, A.A., van Diepen, C.A. (Eds.), 1994. System Description of the WOFOST 6.0 Crop Simulation Model Implemented in CGMS. Publication EUR 15956 EN of the Office for Official Publications of the EU, Luxembourg.
Todorovic, P., Woolhiser, D.A., 1975. A stochastic model of n-day precipitation. J. Appl. Meteorol. 14, 17–24.
Tuller, S.E., Brett, A.C., 1984. The characteristics of wind velocity that favor the fitting of a Weibull distribution in wind speed analysis. J. Climate Appl. Meteorol. 23, 124–134.
van der Voet, P., van Diepen, C.A., Oude Voshaar, J., 1993. Spatial interpolation of daily meteorological data: a knowledge based procedure for the regions of the European Communities. Report 53/3. The Winand Staring Centre–the Joint Research Centre, Wageningen–Ispra, Italy.
van der Wal, T., 1995. Effect of start date on uncertainty of final simulated yield. Wageningen, DLO Winand Staring Centre/JRC. Int. Med. 346, pp. 20.
Wand, S.J.E., Midgley, G.Y.F., Jones, M.H., Curtis, P.S., 1999. Responses of wild C4 and C3 grass (Poaceae) species to elevated atmospheric CO_2 concentration: a meta-analytic test of current theories and perceptions. Global Change Biol. 5 (6), 723–741.
Willekens, A., van Orshoven, J., Feyen, J., 1998. Estimation of the phenological calendar, Kc-curve and temperature sums for cereals, sugar beet, potato, sunflower and rape seed across Pan Europe, Turkey and the Maghreb countries by means of transfer procedures. Vol. 1: Project Report. Contract no: 13118-97-07 F1ED ISP B. Joint Research Centre of the European Communities. Space Applications Institute, MARS, project, Ispra, Italy.
Willekens, A., van Orshoven, J., Feyen, J., 1998. Estimation of the phenological calendar, Kc-curve and temperature sums for cereals, sugar beet, potato, sunflower and rape seed across Pan Europe, Turkey and the Magreb countries by means of transfer procedures. Vol. 1: Project Report. Contract no: 13118-97-07 F1ED ISP B. Joint Research Centre of the European Communities. Space Applications Institute, MARS, project, Ispra, Italy.
Wilks, D.S., 1992. Adapting stochastic weather generation algorithms for climate changes studies. Climate Change 22, 67–84.
Wilks, D.S., 1998. Multisite generalization of a daily stochastic precipitation generation model. J. Hydrol. 210, 178–191.
Wilks, D.S., 1999. Interannual variability and extreme-value characteristics of several stochastic daily precipitation models. Agricult. Forest Meteorol. 93, 153–169.
Wilks, D.S., Wilby, R.L., 1999. The weather generation game: a review of stochastic weather models. Prog. Phys. Geograp. 23, 329–357.
Wolf, J., van Oijen, M., 2002. Modelling the dependence of European potato yields on changes in climate and CO_2. Agric. Forest Meteorol. 112, 217–231.
Wolf, J., van Oijen, M., Kempenaar, C., 2002. Analysis of the experimental variability in wheat responses to elevated CO_2 and temperature. Agricult. Ecosyst. Environ. 93, 227–247.
Wolf, J., van Oijen, M., 2003. Model simulation of effects of changes in climate and atmospheric CO_2 and O_3 on tuber yield potential of potato (cv Bintje) in the European Union. Agricult. Ecosyst. Environ. 94, 141–157.
Woolhiser, D.A., Roldan, J., 1982. Stochastic daily precipitation models: 2. A comparison of distribution of amounts. Water Resour. Res. 18, 1461–1468.